André Luís Teixeira Gutierres

BSc in Biochemistry

Structural and functional studies on human enzymes involved in hydrogen sulfide breakdown

DISSERTATION FOR OBTAINING THE MASTER'S DEGREE IN BIOCHEMISTRY

Supervisor: Dr. João B. Vicente, ITQB-UNL

Co-Supervisor: Dra. Margarida Archer, ITQB-UNL

Co-Supervisor: Dr. José Artur Brito, ITQB-UNL

[September 2016]

FACULDADE DE CIÊNCIAS E TECNOLOGIA
UNIVERSIDADE NOVA DE LISBOA

André Luís Teixeira Gutierres

BSc in Biochemistry

Structural and functional studies on human enzymes involved in hydrogen sulfide breakdown

DISSERTATION FOR OBTAINING THE MASTER'S DEGREE IN BIOCHEMISTRY

Supervisor: Dr. João B. Vicente, ITQB-UNL

Co-Supervisor: Dra. Margarida Archer, ITQB-UNL

Co-Supervisor: Dr. José Artur Brito, ITQB-UNL

[September 2016]

FACULDADE DE CIÊNCIAS E TECNOLOGIA
UNIVERSIDADE NOVA DE LISBOA

Acknowledgment

After a long journey, it is time to thank who was with me. First of all, a great thank to my fathers and brother, for supporting me all this time and to make sure I gave my best.

A great thank to Professora Doutora Maria Arménia Carrondo for letting me be part of your research group.

A huge thank to the research group partner of Rhodanese and SQR work, Alessandro Giuffrè and Francesca Malagrinò for the amazing collaboration.

The same compliment to Tiago M.Bandeiras and Paulo Espirito Santo for the work on CBS.

A thanks to Dr. Katsuaki Inoue for the collaboration on SAXS.

A great acknowledgement to all the people that belongs to the laboratory group, namely Denise, Karim, Patricia, Rute, Sandra and Sara.

A thank you to Dr. Pedro Matias, Dra. Elin Moe, Dr. Colin McVey, Dra. Célia Romão and Dr. Carlos Frazão for the spread of knowledge.

A thank you to Diogo, Ines and Maria from the laboratory of membrane protein crystallization.

An acknowledgement to all personal of iBet company, namely Micael, Cristiana, Joana and Andreia.

For now, I need to make a great acknowledgement to my two co-supervisors, Dra. Margarida Archer and Dr. José Brito. It was the second time that I work with both and like the first one, I really enjoy to learn from they.

For the last, to my supervisor, João Vicente, for keeping me in the right direction. Helping to understand all the methods that we used on this work, to always be concern if I understand all the steps. Not for the grease, but I learned a lot from him and I hope to see our paths cross again in the future.

In a more personal detail, I need to thank all my friends that helped me during this dissertation, each one at his own way. For that, I thank to Ana, Beatriz, Diana, Daniela, Filipa, Mariana, João D., Filipe, Hugo, David S., João S., Patrick, Mário, João R., Ricardo, Rui, João L., Tiago, Ricardo S., João G., Rodrigo.

To all, a big and sincere thank you.

Abstract

In human physiology, hydrogen sulfide (H_2S), a small gaseous molecule that diffuses across aqueous and hydrophobic milieu, has been shown to team up with NO and CO as the third 'gasotransmitter'. The still growing number of physiological processes shown to be regulated by H_2S includes blood flow, cellular stress response, inflammation, immune defense, apoptosis and energy metabolism.

Consequently, disturbed H_2S metabolism is associated with numerous human pathologies, from cardiovascular and inflammatory disorders, to neurodegeneration and cancer. As any other reactive signaling molecule, H_2S homeostasis requires a fine balance between its synthesis and breakdown. One of the enzymes involved in the synthesis of H_2S in humans is cystathionine β-synthase (CBS), one key enzyme of the transsulfuration pathway. H_2S breakdown relies on a mitochondrial pathway involving a sulfide:quinone oxidoreductase (SQR), a sulfur dioxygenase, Rhodanese, and a sulfite oxidase. O_2-dependent H_2S consumption may be primarily controlled by its efficient catabolism via SQR, which may be a key regulator in switching off H_2S signaling by consuming it.

Although numerous studies have focused on the functional analysis of H_2S catabolism components, there is a paucity of structural data to support i) the understanding of functional/physiological data, and ii) the discovery and design of modulatory compounds with potential pharmacological interest.

The aim of this dissertation was to characterize from a structural and functional viewpoint human enzymes involved in H_2S metabolism, employing different biophysical methodologies.

Recombinant human Rhodanese was expressed in *Escherichia coli* and purified with a yield of 2mg/L of culture. By a combination of DSF (Differential Scanning Fluorimetry), CD (Circular Dichroism) and SAXS (Small Angle X-ray Scattering) studies, it was observed that cysteine, thiosulfate and alliin affects Rhodanese structure. This information was used into crystallization trials but without getting any Rhodanese crystals. The recombinant human SQR expression and purification was unsuccessful, precluding any further studies, and being still under development.

In parallel with work on the sulfide oxidizing unit, structural studies were carried out with recombinant human cystathionine β-synthase. In particular, the crystallographic structure of the disease-causing variant CBS P49L was obtained at 2.8 Å resolution, showing very subtle differences from the WT CBS structure. However, these do not completely explain the functional impact of this mutation and its pathogenicity.

Resumo

Na fisiologia humana, o sulfato de hidrogénio (H_2S), uma pequena molécula gasosa que difunde pelo meio aquoso e hidrofóbico, foi demonstrado que pertence à família dos 'gasotransmissores' como o NO e o CO. O numero de processos fisiológicos regulados pelo H_2S continua a aumentar e entre eles inclui-se o fluxo sanguíneo, resposta ao stress celular, inflamação, imunidade, apoptose e metabolismo energético.

Consequentemente, distúrbios no metabolismo do H_2S esta relacionado a muitas patologias humanas, desde cardiovascular e desordens inflamatórias até neurodegeneração e cancro. Como outras moléculas de sinalização reativas, H_2S homeostase requer um balanço perfeito entre a sua síntese e a sua degradação. Uma das enzimas envolvidas na síntese de H_2S é a cistationina β-sintase (CBS), uma enzima chave na via anabólica. A degradação de H_2S baseia-se numa vida metabólica mitocondrial que envolve a sulfato:quinona oxidoreductase (SQR), uma dioxigenase de enxofre (Rhodanese) e uma sulfito oxidase. Os níveis de H_2S podem ser controlados pela via catabólica que envolve a SQR, que pode ser a chave no processo de sinalização pelo H_2S, visto que pode consumir a molécula.

Apesar dos vários estudos terem-se focados na analise do catabolismo do H_2S e seus componentes, há uma falta de dados estruturais que suporta i) o entendimento dos dados sobre a função e fisiologia e ii) descobrir e desenhar compostos modulatórios que possam ter um potencial farmacêutico interessante.

O objetivo desta Tese foi caracterizar de um ponto de vista estrutural e funcional enzimas humanas envolvidas no metabolismo do H_2S, empregando diferentes metodologias.

Rhodanese recombinante humana foi expressa em *Escherichia coli* e purificada com um rendimento de 2mg/L de cultura. A expressão e purificação da SQR recombinante humana foi um insucesso, impedindo qualquer estudo posterior, estando ainda sobre desenvolvimento. Foi demonstrado por ensaios de DSF, CD e SAXS que, na presença de cisteína, tiossulfato e alliin, a Rhodanese sofre modificações na sua estabilidade global, sendo esta informação explorada para ensaios cristalográficos. Mesmo com toda esta informação, não foi possível obter cristais de Rhodanese.

Em paralelo com o trabalho em enzimas da oxidação do sulfureto, estudos estruturais foram realizados na CBS recombinante humana. Em particular, a estrutura cristalina de uma mutação causadora de doença CBS P49L, obtida com uma resolução de 2.8 Å, demonstrando diferenças muito subtis em relação à sua forma natural, o que não permite concluir o impacto funcional e a patogenicidade desta mutação.

Objectives

The main goal of this dissertation was to structurally characterize human enzymes involved in hydrogen sulfide metabolism.

The detailed objectives of this work were as follows:

1. Purification of recombinant human Rhodanese and sulfide:quinone oxidoreductase (SQR);
2. Screening for compounds with a structural-functional effect towards the target proteins;
3. Validating the selected compounds by biophysical methodologies;
4. Obtaining the crystallographic structures of the target enzymes, particularly Rhodanese, SQR and CBS (WT and P49L mutant);

Keywords

Hydrogen Sulfide (H_2S)

Sulfide:quinone Oxidoreductase (SQR)

Rhodanese (Rhod)

Cystathionine β-synthase (CBS)

X-ray crystallography

Small Angle X-ray Scattering (SAXS)

Circular Dichroism (CD)

Differential Scanning Fluorimetry (DSF)

Abbreviations

RNA: Ribonucleic acid

3D: 3-Dimensional

PDB: Protein Data Bank

Cys: Cysteine

DNAses: deoxyribonuclease

HEPES: 4-(2-hydroxyethyl)-1-piperazineethanesulfonic acid

$MgCl_2$: Magnesium Chloride

E.coli: *Escherichia coli*

Rpm: rotations per minute

NaCl: Sodium Chloride

SDS-PAGE: Polyacrylamide gel electrophoresis

DMSO: Dimethyl sulfoxide

PEG: Polyethylene glycol

ESRF: European Synchrotron Radiation Facility

Tm: Melting Temperature

Index

Index of Figures

Index of Tables

1. – Introduction

1.1 – Sulfur chemistry

Sulfur, represented by the atomic symbol S and with an atomic number of 16 in the Periodic Table of the elements [1], has an atomic weight of 32.06 [2]. Sulfur is the 16th more abundant element in Earth's crust, with a percentage of 0.034% [3] and exists in different valence states from -2 (as in H_2S) to +6 (as in SO^{4-}).

From the biological point of view, sulfur is present in vitamins, hormones and the amino acids methionine and cysteine. Hence, it is one of the most important compounds in human biology belonging to the group CHNOPS – Carbon, Hydrogen, Nitrogen, Oxygen, Phosphors, Sulfur – considered the six more important chemical elements in human life [4]. In human physiology, sulfur plays a major role in some specific metabolic processes. Regarding the two amino acids mentioned above that contain sulfur in its composition, methionine cannot be synthesized by the human body, so it has to be taken up through the diet. On other hand, cysteine can be synthesized *de novo*. Since the human body is not capable of storing sulfur, it needs to be oxidized to sulfate, excreted in the urine or stored in the form of glutathione (GSH), a powerful body antioxidant [5].

Besides human physiology, sulfur is present in several other biological processes within the sulfur cycle, consisting of moving sulfur from minerals to living systems [6].

1.2 - Sulfur Cycle

The sulfur cycle (Figure 1.1) comprehends 3 major steps: firstly, the mineralization of organic sulfur into inorganic species, like hydrogen sulfide (H_2S); secondly, the oxidation to sulfate (SO_4^{2-}); and, finally, the re-reduction to H_2S.

Sulfur in the presence of oxygen yields sulfur dioxide (SO_2). This compound reacts with water, producing sulfuric acid (H_2SO_4) that evaporates to the atmosphere and returns in the form of acid rain, to be absorbed by plants and restart the cycle [7]. Microorganisms have an important role in the sulfur cycle since they are responsible for the converting of organic sulfur into inorganic.

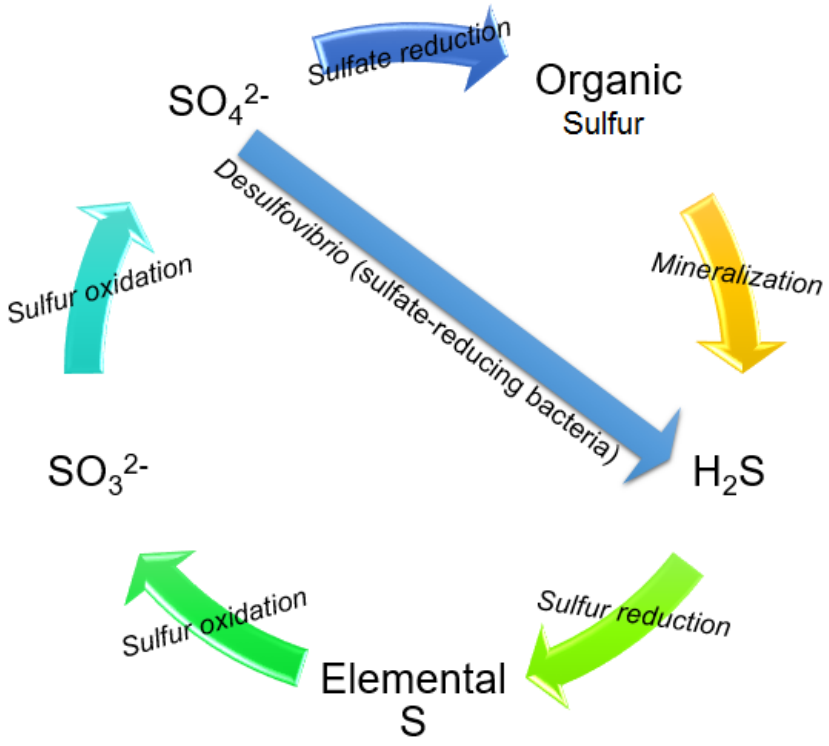

Figure 1.1 – Sulfur cycle. Sulfate (SO_4^{2-}) is reduced in to organic sulfur or by action of gut bacteria, converted to hydrogen sulfide (H_2S). The organic sulfur can also be converted to hydrogen sulfide by a mineralization process. Hydrogen sulfide is reduced to elemental sulfur (S^0) and the cycle goes on a sulfur oxidation to form an intermediate sulfur trioxide (SO_3^{2-}) and the final product sulfate.

1.3 – Hydrogen Sulfide (H_2S)

Hydrogen sulfide (H_2S) plays an important role in human physiology since it acts as a signaling molecule regulating multiple physiological processes [8]. Different studies have demonstrated that H_2S, besides being a toxic gas, is an important molecule in human physiology. H_2S is in equilibrium with hydrosulfide (HS^-) and sulfide (S^{2-}), as shown by the $pK_a1{\sim}7(H_2S/HS^-)$ and $pk_a2{\sim}19(HS^-/S^{2-})$, at 25ºC. In human blood, where the pH is 7.4, HS^- is the more abundant specie (70-80%), whereas H_2S is only around 20-30% and S^{2-} is present in negligible quantities. From now on, the term "H_2S" and "sulfide" are related to each other as the H_2S/HS^- pair [9].

H_2S is considered a gasotransmitter molecule like nitric oxide (NO) and carbon monoxide (CO) [10], all the three with major roles in physiological processes. Studying the mechanisms of hydrogen sulfide synthesis, its regulation and distribution across cells and tissues was useful to further understand various pathologies directly related to H_2S metabolism (like colon cancer, atherosclerosis and diabetes) [11]. There are two major pathways for H_2S production: through endogenous enzymes, and through the gut microbiota.

In the endogenous pathway, there are three enzymes responsible for the H_2S production: the methionine metabolism cystathionine β-synthase (CBS), cystathionine γ-lyase (CGL) and 3-mercaptopyruvate sulfurtransferase (MST) [12]. Regarding gut microbiota, sulfate-reducing bacteria (SRB) represent approximately 50% of the microbial colonization of human gut [13]. These bacteria (including members of the genus *Desulfovibrio*) consume H_2 or organic compounds and the electrons from that reaction are used for the reduction of sulfate into H_2S. SRB are associated with inflammatory bowel diseases, and there is recent evidence that H_2S generated by SRB mediates the inflammation process [14].

1.4 – Hydrogen Sulfide formation in Human Metabolism

Human H_2S metabolism is mostly related with the methionine cycle. This cycle starts with the methionine conversion to S-adenosylmethionine (SAM or AdoMet), catalyzed by the enzyme methionine adenosyltransferase (MAT) [15]. SAM is the methyl donor for virtually all methylation reactions in human physiology. Once it donates the methyl group through various methyltransferases, it is converted into S-adenosylhomocysteine (SAH). In the next step, SAH loses its adenosyl group through a hydrolysis reaction catalyzed by SAH hydrolase. After this step, homocysteine can either enter the transsulfuration pathway or be re-methylated back to methionine. The transsulfuration pathway produces cysteine through enzymes CBS and CGL (Figure 1.2).

CBS catalyzes the condensation of homocysteine with serine to form cystathionine (details for the CBS protein are given below). CGL catalyzes the breakdown of cystathionine into cysteine and α-ketoglutarate. CGL belongs to the pyridoxal 5'-phosphate (PLP)-dependent enzymes, constituted by two main domains, a large PLP-binding domain (the active site) and a smaller domain [17]. It is known for this CGL enzyme the capability of generating H_2S using cysteine alone or together with homocysteine [18]. Noteworthy, CBS can also use the same compounds to generate H_2S [16]. The CGL gene may suffer some mutations that can cause cystathioninuria, a disease related to the accumulation of cystathionine in blood or tissues and that may contribute to mental disorders [19].

Besides H_2S-generating enzymes of the transsulfuration pathway, another pathway leads to H_2S synthesis. Cysteine can be converted to 3-mercaptopyruvate (3-MP) by cysteine aminotransferase (CAT), a PLP-dependent enzyme also named glutamate oxaloacetate transaminase (GOT). The last enzyme is 3-mercaptopyruvate sulfurtransferase, MST, that catalyzes the conversion of 3-mercaptopyruvate into H_2S, through a cysteine active site [20]. This enzyme belongs to the family of sulfurtransferases, has 60% sequence similarity with another enzyme involved in the H_2S breakdown (Rhodanese), and a molecular weight of 34 kDa. MST has two domains and the local active site where 3-MP binds is located between these two domains [21].

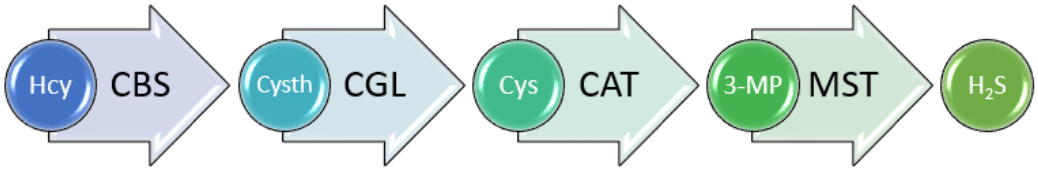

Figure 1.2 – Completed human H_2S production pathway. CBS catalyzes homocysteine conversion to cystathionine, then CGL catalysis the cysteine formation with CAT responsible for the catalyze into 3-MP and finally MST catalyzes the conversion into H_2S.

1.5 – Hydrogen Sulfide breakdown in Human Metabolism

Since high H_2S levels can be harmful to human welfare, a sulfide breakdown pathway is necessary [22]. This catabolic pathway is known as the sulfide oxidizing unit (SOU) and its main objective is the conversion of H_2S into thiosulfate ($S_2O_3^{2-}$) and/or sulfate (SO_4^{2-}) in order to be eliminated from the body in the urine. There are four known enzymes involved in this pathway: Sulfide:Quinone Oxidoreductase (SQR), Sulfur Dioxygenase (ETHE1), Rhodanese (Rhod) and Sulfite Oxidase (SOx). All these enzymes are within the mitochondria and SQR may, under special conditions, supply electrons for the mitochondrial oxygen respiration electron transfer chain [23]. The SQR enzyme, a flavoenzyme, catalyzes the conversion of H_2S and glutathione into glutathione persulfide (GSSH) [24] while transferring the electron equivalents to ubiquinone [25]. These electrons can then be fed into complexes III and IV. SQR can be related to oxygen respiration and the enzyme is essential to the human H_2S breakdown so this enzyme plays an essential role of maintaining H_2S levels in a restricted range, since at lower concentration it feeds the mitochondrial electron transfer chain involved in oxygen respiration. Higher levels of H_2S can leaves to all complex inhibition.

The second enzyme in the pathway, ETHE1, is a 54 kDa metalloenzyme that catalyzes the conversion of GSSH into sulfite (SO_3^{2-}) using oxygen as co-substrate [26]. Mutations in the ETHE1-encoding gene are directly related to the disease ethylmalonic encephalopathy (that affects mainly the nervous system). SO_3^{2-} can then follow two different routes [27], one of which is catalyzed by Rhodanese (Figure 1.3) to produce $S_2O_3^{2-}$ (also using GSSH as co-substrate). Rhodanese is an important study target because of its importance in some cellular mechanisms like the moving of 5S ribosomal RNA into human mitochondria [28]. Rhodanese belongs to the family of transferases and, so far, there is no information about the human enzyme structure, although some functional studies have already been published. One important known function is cyanide detoxification. Some studies have also shown that alterations in the Rhodanese-encoding gene are related to inflammatory bowel diseases [29].

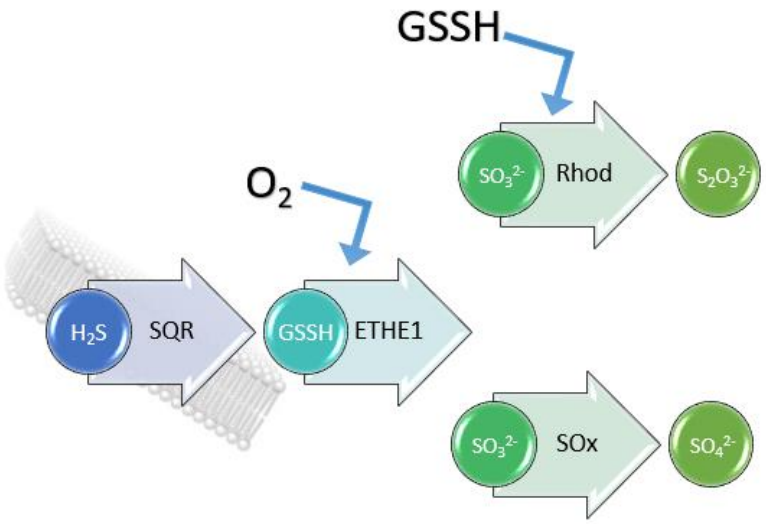

Figure 1.3 – H_2S breakdown pathway. Starts with the formation of GSSH in the presence of the enzyme SQR. Then oxygen dependent enzyme ETHE1 catalyzes the conversion to SO_3^{-2} and then, two routes possible to follow: One, Rhod in the presence of GSSH catalyzes the conversion to $S_2O_3^{2-}$ or SOx catalyzes the conversion to SO_4^{2-}.

SO_3^{2-} can also be oxidized to SO_4^{2-} by SOx (Figure 1.3). In the human body, this enzyme functions as a homodimer. On the N-terminus, a heme *b* cofactor is present while in the C-terminus is present a molybdopterin cofactor (with a molybdenum center), the site of sulfite oxidation [30].

This project focuses on the structural and functional studies of three enzymes that are part of the H_2S metabolism: Cystathionine β-synthase (CBS), sulfide:quinone oxidoreductase (SQR) and Rhodanese (Rhod).

1.6 – Human Cystathionine β-synthase (CBS) enzyme

CBS is the first enzyme of the transsulfuration branch of methionine metabolism, catalyzing the conversion of homocysteine and serine to cystathionine [31]. Human Cystathionine β-synthase (hCBS) is considered an homotetrameric enzyme, each subunit having a molecular weight of 63 kDa, and with three major domains: The N-terminal region harboring a *b*-type heme, one catalytic core with the cofactor pyridoxal-5'-phosphate (PLP) and a regulatory C-terminal domain responsible for enzyme allosteric regulation [32]. The C-terminal domain has a major role on the activation or inhibition of this enzyme, containing a pair of CBS motifs (conserved structural domains) where the activator S-adenosylmethionine (AdoMet) binds. This region is also called "Bateman module" because of the assumed shape and it is considered to be responsible for CBS tetramerization [33].

The structural conformation of the basal form of CBS hampers substrate access to the catalytic core. When the activator AdoMet binds to the regulatory domain, the enzyme changes its domain arrangement and the catalytic core opens to substrate binding. Low CBS activity can cause some disturbances on the normal pathway and can lead to certain diseases like thrombosis and vascular disease [34]. The *cbs* gene can suffer some mutations that alter enzyme activity and protein folding and stability [35] and can cause classical homocystinuria, a disorder in the metabolism of methionine that affects the nervous and vascular systems [36]. Some CBS mutations also affect AdoMet activation, either by increasing the rate of activation or inhibiting its binding. Herein was studied a disease-causing variant, P49L, which affects protein function, without any influence on the AdoMet activation [37].

Despite the importance of CBS in the hydrogen sulfide metabolism, it has been demonstrated that an inhibition of CBS will not stop H_2S production since CGL has the capacity to produce H_2S by itself [38]. The inhibition of CBS enzyme can be caused by the other two gasotransmitters, NO and CO [39].

.

1.7 – Human sulfide:quinone oxidoreductase (SQR) enzyme

SQR belongs to the flavoprotein disulfide oxidoreductases family. Like the enzymes of this family, SQR is thought to have two redox centers: one cysteine disulfide and a flavin adenine dinucleotide (FAD), which transfers electrons to the quinone pool. SQR is bound to the mitochondrial membrane [40]. One of the objectives of this work was to obtain the crystallographic structure of human SQR. Until today, studies have demonstrated that SQR has an important role in maintaining low intracellular H_2S levels below toxic [41]. Besides the conversion reaction of H_2S to glutathione persulfide (GSSH), another reaction that involves SQR is the reduction of ubiquinone into ubiquinol, using the electrons released from H_2S oxidation.

Although there is no 3D structure of human SQR, there are some structures of different organisms published, as for example, from *Acidianus ambivalens* [42]. That information can be used to predict a model for the human SQR (Figure 1.4). Although having a low sequence similarity (~30%), the crystallographic structure of SQR from *Acidithiobacillus ferrooxidans* (PDB ID: 3SZF) was used as a template.

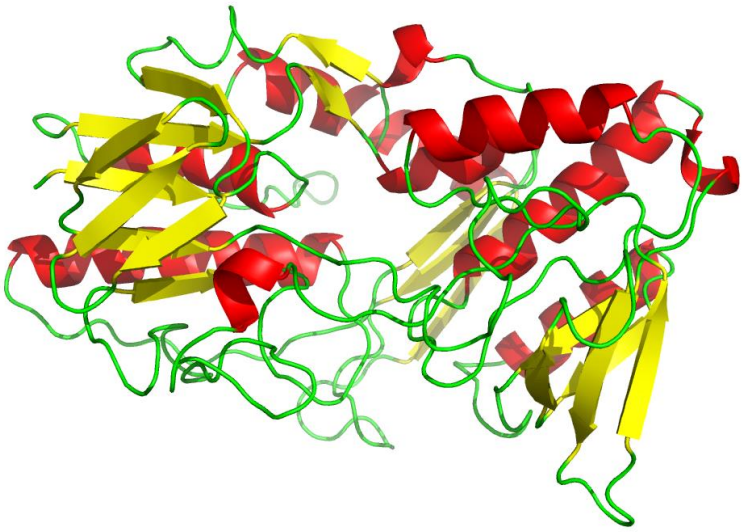

Figure 1.4 – Human SQR 3D structure modelling using the Swiss-model server [47]. The template has ~19% sequence identity (SQR from Acidithiobacillus ferrooxidans, PDB code: 3SZF [43]).

1.8 – Human Rhodanese (Rhod) enzyme

Although the crystallographic structure of human Rhodanese has not yet been reported, Rhod is an enzyme very well functionally studied. In early days, the only known role for this enzyme was the detoxification of cyanide, particularly the conversion of thiosulfate and cyanide to thiocyanate and sulfite. For this reason, it was attributed the name of thiosulfate:cyanide sulfurtransferase and can be used as an antidote for cyanide poising [44]. The role of Rhod in the sulfide oxidizing unit was only found in later studies. An interesting fact is the possibility of this enzyme to have a reversible reaction mechanism. Rhod major role is the $S_2O_3^{2-}$ production but can also produce GSSH with less efficiency. Any changes in the Rhodanese-encoding gene can be related to certain diseases like ulcerative colitis and influence the nervous system [45].

In the absence of a crystallographic structure, only predictions can be made using Rhod from different organisms with a high sequence identity. Using the structure prediction tool SWISS-MODEL [48], it was possible to generate a 3D model [49].

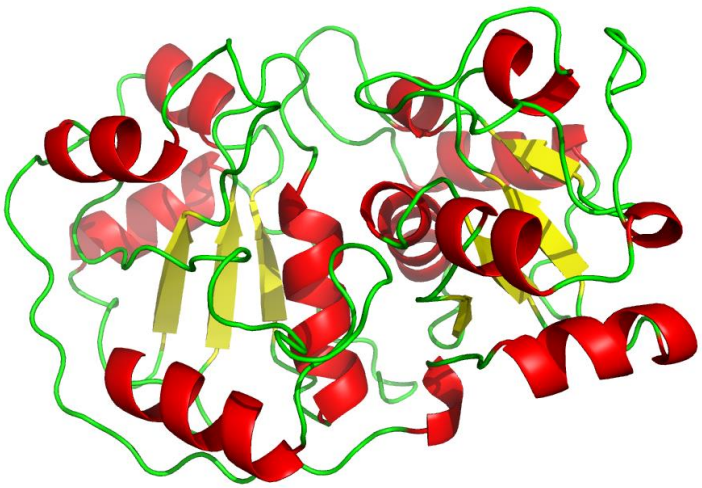

Figure 1.5 – Human Rhodanese 3D structure prediction. Using swiss-model tool [50], the template has 89,53% sequence identity (Rhodanese from Bos taurus, PDB code: 1BOH [46]).

For this prediction, the crystallographic model of bovine Rhodanese (PDB ID 1BOH) was used, with sequence similarity of 59% [46]. This Rhod crystal structure (Figure 1.5) was truncated in the N-terminal domain to check any changes on the conformational stability and the trials indeed demonstrated that the stability is affected. Another finding from this crystal Rhod structure was that the active site residue is Cys247.

2 – Material and Methods

2.1 – Materials

Kanamycin, sucrose and glycerol were purchased from Carl Roth. Tris, lysozyme, DNAses, imidazole, HEPES, ampicillin, gentamicin, TrisAcetate, $MgCl_2$ and Triton X-100 were bought from Sigma Aldrich. IPTG was bought from Apollo and protease inhibitors from Roche. All the compounds used in DSF (Differential Scanning Fluirometry) and CD (Circular Dichroism) assays were bought from Sigma.

2.2 - Expression and Purification of human Rhodanese

A pET28b-based construct containing the codon optimized synthesized gene encoding human Rhodanese cloned between the NcoI and XhoI sites was purchased from Genscript (USA). Competent *E. coli* BL21(DE3) cells were transformed with the Rhodanese expression plasmid. A single colony was used to inoculate 50 ml of Luria Bertani (LB) medium supplemented with 50µL of 50 mg ml^{-1} kanamycin, and grown overnight at 37ºC and 180 rpm. The bacterial culture (40ml) was used to grow 4x1L in LB medium containing 4mL 50 mg ml^{-1} kanamycin, growing at 28ºC and 180 rpm until the $O.D_{600}$ reach 0.5-0.6 (~3 hours). At this point, 400 µL of 1M Isopropyl β-D-1-thiogalactopyranoside (IPTG) were added and temperature and stirring reduced to 16ºC and 120 rpm, respectively, for 18 h. The cells were collected by centrifugation at 7500 rpm for 5 minutes at 6ºC. The cells were stored at -20º.

After thawing, the cells were suspended in lysis solution containing 50 mM TrisHCl pH 8, 500 mM NaCl, 2,5 mg/ml Lysozyme, one tablet protease inhibitors and DNAse and sonicated on ice with a pulse sequence of 30s pulse, 30s rest with a total of 10 minutes. Cell debris were removed by centrifugation at 18000 rpm for 30 minutes at 6ºC.

The first step of purification was an affinity exchange using and HisTrap FF Crude 5ml pre-equilibrated with 50mM Tris pH8 and 500mM NaCl. The elution of Rhodanese was made with a linear gradient from 0 to 500mM of Imidazole. The fractions with Rhodanese were identified by SDS-PAGE and concentrated by ultra-filtration (Amicon®) in a benchtop centrifuge at 5000 rpm, 6ºC. A size exclusion chromatography step was performed in a Superdex 200 gel filtration column (GE Healthcare). Sample was eluted with 100mM HEPES pH7.4 and 150mM NaCl. The fractions with Rhodanese were identified by SDS-PAGE and concentrated. The last purification step was an ionic exchange filtration using a 5-ml HiTrap Q-sepharose FF pre-equilibrated with 20mM TrisHCl pH8. Rhodanese was eluted with a gradient of 0 to 1M of NaCl. Rhodanese was identified by SDS-PAGE, concentrated (Amicon®) and protein concentration was determined by the Bradford method (SIGMA reagent) with the major fraction obtaining 36 mg/ml. Rhodanese final buffer is 20mM TrisHCl pH8 with 60mM NaCl.

2.3 – Differential Scanning Fluirometry (DSF) of Rhodanese

This technique can be used to determine the amount of denatured protein by temperature increase under different conditions [51]. To follow that denaturation, it is necessary to add a dye to the sample, named SYPRO Orange (SIGMA). When the protein starts to unfold due to the applied heat (thermal denaturation), this dye will bind to the exposed hydrophobic regions [52], increasing its fluorescence. Each well has 5µl of an effector (buffer, salt, small molecule), 20µL protein (5µg) and 25µL of SYPRO(20x), in a total of 50µL per well. Each tested condition was made in triplicate.

This 96-well screen assembles several different conditions to test. In these trials, we tested the "apo" form of Rhodanese and incubated with different compounds to compare the behavior. These trials were performed on a BioRad iQ5 RT-PCR Optical System. The different compounds tested were Glutathione, Cysteine, Homocysteine, Thiosulfate, Sulfite, Garlic oil, DMSO, Allyl Sulfide, Alliin, S-allyl-cysteine, S-methyl-cysteine and N-acetyl-cysteine.

2.4 – Circular Dichroism (CD) of Rhodanese

Structural studies can be done with different kind of methods and CD is one of those. It is a method that is based on circular polarized light that diffracts into two different directions [53]. One of this technique purpose is to assess/analyze the secondary structure of proteins and the protein behavior under thermal denaturation. Rhodanese was tested on a range of wavelength from 205nm to 260nm to see the structural variation with the presence of ligands.

Here, this method was used also to test the thermal denaturation, with a specific wavelength of 222nm, where it is possible to evaluate the unfolding of the Rhodanese [54]. Rhodanese in its "apo" form and with three different ligands, cysteine, thiosulfate and alliin. The samples measurement were done all in a Jasco J-815 CD spectrometer equipment.

2.5 – Crystallization of human Rhodanese

X-ray crystallography is one of the most frequent methods to determine the 3D structure of macromolecules. The theoretical concept behind X-ray crystallography is the ability of crystals of protein to diffract X-ray light [55]. However, one of the major bottlenecks of this technique is to obtain good quality, single crystals that can diffract X-rays. Only from these it is possible to obtain a good diffraction pattern to proceed with data collection and all subsequent steps (see below). The concept of crystals is to assure that protein molecules are organized in the same way in a confined space acting as a "signal amplifier" for the X-ray diffraction, where the asymmetric unit multiplied by *x* will form the unit cell [56]. The three dimensional arrangement of *n* unit cell forms the crystal. When the light targets the crystal and is diffracted, originates several diffractions spots. Each spots contain information about all atoms of the molecule, which is characterized by the amplitude (F_{hkl}), related with the number of electrons that each atom contributes and by a phase (α_{hkl}), related with the position of the atoms in the unit cell. Besides the amplitude of each spot, also the relative angle of each spot is necessary to solve, originating the phase problem [57].

This phase problem, today, can be solved by different methods, the most common being Molecular Replacement, which consists of using a known structure to serve as base for the new data. When there is no possible to use a published structure, other methods can be applied, like MIR, MAD and SAD. MIR (Multiple Isomorphs Replacement), consist in introduce a heavy metal, like iron, in the crystal to cause different intensity variation in the diffraction and then compare that information with the without heavy metal. MAD (Multiple Anomalous Dispersion) consist in the anomalous effect caused by the heavy metal when read in different wavelengths. SAD (Single Anomalous Dispersion) is the same as MAD but only with one wavelength [58].

Crystallization trials of Rhodanese were performed in 96-wells Swissci triple drop UV polymer plates (Molecular Dimensions). These trials were performed under controlled humidity at room temperature (20ºC), in a mini-bee Cartesian crystallization robot (Genomic Solutions). Four different conditions were tested - apo-Rhodanese, Rhodanese with TS (Thiosulfate), Rhodanese with Cys (Cysteine) and Rhodanese with Alliin – using several commercially available screenings: Pact Premier (Molecular Dimensions), Footprint (Molecular Dimensions), Structure I & II (Molecular Dimensions), JCSG+ (Molecular Dimensions), MORPHEUS (Molecular Dimensions), Midas (Molecular Dimensions), PGA (Molecular Dimensions) and Clear Strategy (Molecular Dimensions). These screening approach tries to cover different regions of the chemical space and possibly allow to determine initial crystallization conditions, and infer on the solubility of the protein in different pH and precipitants.

2.6 – Bio-SAXS of Rhodanese: Data collection and Processing

Small-Angle X-ray Scattering (SAXS) is a method for the structural characterization of macromolecules in solution. The main information provided by this technique is the size and the shape of the protein "envelope" in solution. It is different from X-ray crystallography since the range of resolution varies between 1nm and 2nm (lower than the resolution provided by X-ray crystallography) [59]. Moreover, the macromolecule is not constrained to a limited space like in the crystal hence providing valuable information regarding mobility, domain arrangement and oligomeric state in solution. Synchrotron X-ray scattering data from human Rhodanese were collected at the B21 beamline (Diamond Light Source, Oxford, UK).

Scattering patterns were measured at protein concentrations ranging from 0.9 to 15 mg/mL. B21 beamline operates in a fixed camera length configuration (4.014 meters) at 12.4 keV, allowing measurements in a resolution range of $0.038 < s < 4.2$ nm^{-1}. Each collected frame results from a 10 second exposure at a wavelength of 1.39 Å (maximum achievable resolution of 2.4 Å). Each curve results from 18 scaled and merged frames, to which 18 scaled and merged buffer backgrounds frames have been subtracted. Data were processed and analyzed using the *ATSAS* software package [60]. The forward scattering I_0 and the radius of gyration R_g were evaluated using the Guinier approximation (Table 3.3). The maximum dimensions D_{max} (Table 3.3) were calculated with SAS Data Analysis Primusqt using AutoGNOM, also determining the distance distribution functions p(r). Low-resolution shape analysis of human Rhodanese in the absence or presence of the tested effector compounds (cysteine and thiosulfate) was performed using the *ab initio* program *DAMMIN* [61], which represents the protein as an assembly of densely packed beads.

2.7 – Crystallization of cystathionine β-synthase (CBS)

Two different forms of CBS were crystalized. One truncated form (ΔC-Terminus) of the wild type enzyme and another truncated form (ΔC-Terminus) harboring the mutation P49L. The crystallization conditions are different for the two. In the case of the wild type, the optimized conditions were: 0.6µL CBS at 26.5 mg/mL plus 0.4µL reservoir solution in a cryschem plate using the sitting drop vapor diffusion technique. The reservoir consists of 500uL of 18%PEG3350, 0.2 M K/Na tartrate and 0.1M Bis-Tris propane pH7.5. For the P49L mutation, the crystallization conditions were: 0.6µL CBS at 27.4 mg/mL plus 0.4µL reservoir solution consisting of 35% PEG2000 MME and 0.15M NaBr. Drops were setup at 20ºC.

2.8 – Model building of cystathionine β-synthase (CBS)

Cryoprotection conditions for diffraction experiments were achieved by transferring the crystals to a 3 µl drop of 35% PEG 2000MME, 5% glycerol, 0.15M NaBr. The crystals were flash-cooled by quick plunging into liquid nitrogen. A single crystal was used for data collection under a nitrogen-gas stream (Oxford Cryosystems 700) on beamline ID30A-3 at the ESRF synchrotron (Grenoble, France) using a PILATUS 6M detector (Dectris) at a wavelength of 0.9677 Å. After indexing and calculation of a data collection strategy using EDNA, a wedge of 360º of data was collected using. The data set was indexed and integrated with *XDS* [62] space-group assignment was performed with *POINTLESS* [63] and scaling was performed with *AIMLESS* [64] all within the *autoPROC* data-processing pipeline [65].

At this stage an R_{free}-flag set was created in each data set corresponding to 5 % of the measured reflections for this data-set. Crystal belong to the monoclinic space group *P*1 with unit cell parameters a = 86.2 Å, b = 86.8 Å, c = 97.8 Å, α = 102.6°, β = 103.1°, γ = 111.2°. Data were truncated at 2.80 Å, for the P49L variant and at 2.4 Å for the WT. Reduction statistics are presented in Table 2.1. The CBS P49L mutant structure was solved by molecular replacement using 1JBQ devoid of any solvent and cofactors as search model. Based on the Matthews coefficient, the search was performed for six molecules. Initial refinement rounds were carried out with *BUSTER-TNT* [66] using the macro that accounts for missing parts of the model.

At this point, electron density features attributed to the heme moieties were easily identified. Iterative cycles of manual model building with *COOT* [67] and refinement are in progress.

Table 2.1 – Data collection and refinement statistics

	CBS "P49L"
Beamline	ID30 (ESRF – Grenoble,France)
Wavelength (Å)	0.9677
Resolution range (Å)	76.4 – 2.8 (2.9 – 2.8)
Space group	*P*1
Unit cell	
a,b,c (Å)	86.2, 86.8, 97.8
α,β,γ (°)	102.6, 103.1, 111.2
Total reflections	121 036 (1126)
Unique reflections	58889 (562)
Multiplicity	2.1 (2.0)
Completeness (%)	98.5 (95.9)
Mean I/sigma (I)	4.9 (1.5)
Wilson B-Factor	41.57
Mosaicity	0.24
R_{merge}	13.0 (54.5)
R-$_{meas}$	17.2 (72.4)
R_{pim}	11.1 (47.2)
$CC_{1/2}$	97.6 (62.1)
R-$_{Work}$ (%)	20.4 (29.3)

R-Free (%)	23.8 (32.4)
Number of non-hydrogen atoms	16391
Macromolecules	15781
Ligands	348
Protein residues	2063
RMS (bonds) (Å)	0.013
RMS (angles) (°)	1.69
Ramachandran favored (%)	97.0
Ramachandran outliers (%)	0.8
Rotamer outliers (%)	2.1
Clashscore	2.79
Average B-Factor	45.41
Macromolecules	45.77
Ligands	41.25
Solvent	29.67

2.9 – Expression and Purification of Sulfide:quinone oxidoreductase (SQR)

A pET23a-based construct containing the codon optimized synthesized gene encoding human SQR was purchased from Genscript (USA). Competent *E. coli* BL21 Arctic cells were transformed with the SQR expression plasmid. A single colony was used to inoculate in 50mL LB medium supplemented with 25µL of 200µM ampicillin and 25µL of 20µM gentamicin and grown overnight at 37ºC and 180 rpm. The bacterial culture (40ml) was used to grow 4x1 liters of Terrific Broth (TB) medium containing 2000 µL of 200µM ampicillin, growing at 28ºC and 150 rpm until the $O.D_{600}$ reach 1.2-1.3. At this point, the bacterial culture was moved to 15ºC and 150 rpm until the $O.D_{600}$ reach 1.5-1.6. When achieved, 2000 µL of 1M Isopropyl β-D-1-thiogalactopyranoside (IPTG) were added maintained the temperature and agitation overnight. The cells were collected by centrifugation at 7500 rpm for 5 minutes at 6ºC. The cells were stored at -20ºC.

Upon thawing, the cells were suspended in lysis solution containing 50mM Tris Acetate pH7.6, 500mM sucrose, 20mM Imidazole, 5mM $MgCl_2$, lysozyme, DNAse and one tablet of protase inhibitors. The cell suspension was disrupted using a French Press with 690-720 bar gap. The cell suspension was centrifuged using a JA-10 rotor at 7500 rpm and 6ºC for 10 minutes. The volume obtained was the reference to add the same volume of a solution containing 50mM KPi pH7.4, 4% (V/V) Triton X-100; 10% (V/V) glycerol and 100mM NaCl and stirring for 2 hours at 4ºC. The cell suspension was centrifuged using a rotor JA-20, 19000 rpm for 30 minutes at 6ºC. To each 100mL of cell suspension, was added 8.5mL of TrisHCL 1M, 5.8 mL of NaCL 5M and 600 µL of Imidazole 2M.

For protein purification, the first step was an affinity exchange using an HisTrap FF Crude 5ml pre-equilibrated with 50mM Tris pH8, 0.5% (Triton X-100, 300mM Nacl and 20mM imidazole. The elution of SQR was made with a linear gradient from 0 to 500mM of Imidazole. The fractions with SQR were identified by SDS-PAGE, concentrated and dialyzed overnight against 2L of 50mM Tris pH8, 0.3% Triton X-100 (V/V) and 5% glycerol (V/V). The second purification step was an anionic exchange using a HiTrap Q FF 5ml pre-equilibrated with 50mM Tris pH8, 0.1% Triton X-100 and 5% Glycerol. The elution of SQR was made with a linear gradient from 0 to 1M of NaCl. The fractions with SQR were identified by SDS-PAGE and concentrated. The third purification step was a size exclusion Superdex 200 gel filtration, eluted with 20mM Tris pH8, 300mM NaCl, 0.1% Triton X-100 (V/V) and 5% glycerol (V/V). SQR was identified by SDS-PAGE, concentrated and dialyzed overnight against 4L of 50mM Tris pH8, 0.3% Triton X-100 (V/V) and 5% glycerol (V/V). The last purification step was a RESOURCE Q pre-equilibrated with 50mM Tris pH8, 0.1% Triton X-100 (V/V) and 5% Glycerol (V/V). The elution of SQR was made with a linear gradient from 0 to 1M of NaCl. The fractions with SQR where identified by SDS-PAGE and concentrated.

3 – Results and Discussion

3.1 - Expression and Purification of Rhodanese

Recombinant human Rhodanese was expressed and purified as reported in *Lybiad et. al* [27]. *Escherichia coli* BL21(DE3) was the used host cell since it is one of the most common expression strains and it proved to be efficient [68]. The first purification step was a metal affinity chromatography, more precisely, a HisTrap [69]. The Rhodanese-encoding plasmid was designed to include a 6xHis-tag on the protein N-terminus, thus allowing to use this type of affinity column.

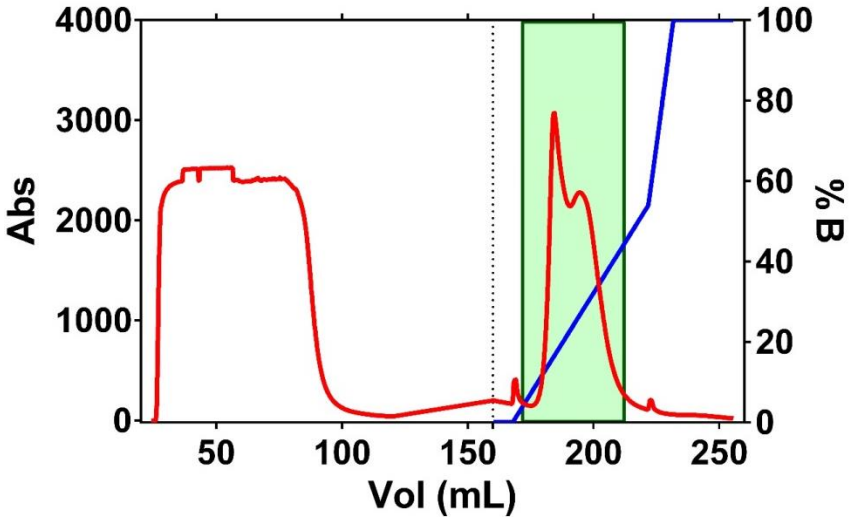

Figure 3.1 – Chromatogram of Rhodanese affinity chromatography. Purification conditions were: Flow 3mL/min, 10mL for fraction. Gradient start represented by dotted line, with a flow 4mL/min, 4ml for fraction. Fractions in the green box were collected. Used column with a total volume of 5mL. 5x upscale on the gradient.

Imidazole was added to the binding buffer to prevent non-specific binding of other contaminant proteins present in the bacterial cell [70]. The eluted fractions were analyzed by SDS-PAGE (Appendix 1) and the Rhodanese-containing fractions (green box in Figure 3.1) were pooled into Fraction R1. The SDS-PAGE showed that Fraction R1 has several contaminant proteins. The next step was a size-exclusion chromatography, allowing to separate the molecules present in solution by their size [71].

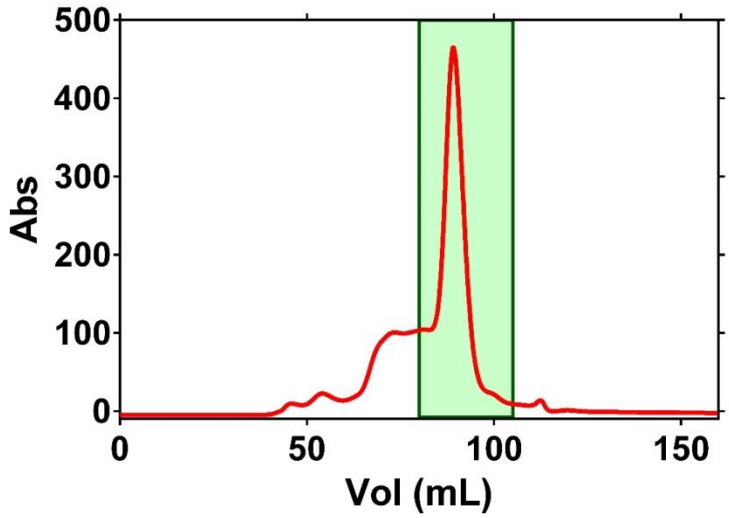

Figure 3.2 – Chromatogram of Rhodanese Size-exclusion chromatography. Purifications conditions were: Flow 0,8mL/min, collecting 2mL for fraction. All fraction on the green box were collected for analyze. Used column with a total volume of 120mL.

The eluted fractions were analyzed by SDS-PAGE and the Rhodanese-containing fractions were pooled and designated as Fraction R1A (Appendix 2). The SDS-PAGE revealed the presence of Rhodanese with some contaminants, not completely pure for crystallization trials. So, for that reason, a third purification step it was necessary, namely an anionic exchange chromatography [72].

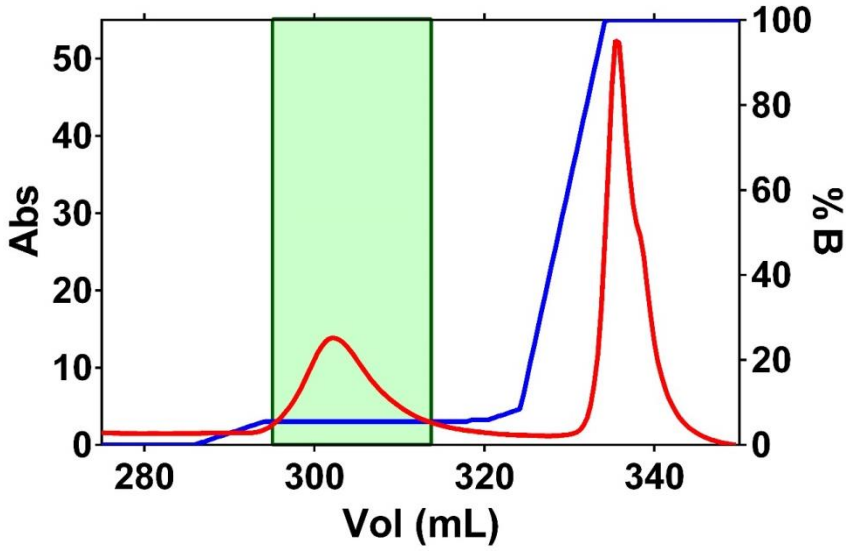

Figure 3.3 – Chromatogram of Rhodanese anionic-exchange chromatography. Purifications conditions were: Flow 5mL/min, collecting 2,5mL for fraction with hold on 6% bidding buffer. All fraction on the green box were collected for analyze. Used column with a total volume of 5mL. 6% bidding buffer with 2x scale.

After dialysis to lower the ionic strength, Fraction R1A was loaded onto the anionic exchange Q-Sepharose column. A linear gradient up to 1M NaCl was employed, and at 60 mM NaCl a hold step was applied. Once the first protein peak eluted, the gradient was resumed and a second peak eluted. The two protein peaks were analyzed by SDS-PAGE, allowing to establish that the first eluted peak corresponds to pure Rhodanese (Appendix 3), whereas the second peak corresponds to the contaminant proteins. Rhodanese was concentrated and quantitated by the Bradford method [73]. Rhodanese yield is calculated as 2 mg Rhod/L of culture.

After purification, a biochemical and biophysical characterization of Rhodanese can be undertaken. The main objective of this work is to get the first crystallographic structure of human Rhodanese. Initial trials were made but without success. Characterization of Rhodanese by other methods could provide information for crystallization.

3.2 - Biophysical characterization

3.2.1 - Differential Scanning Fluorimetry (DSF) of Rhodanese

Since the initial crystallization trials were not successful, the major objective was to search some compounds that could help the crystallization of Rhodanese. To do that, DSF assays were performed in search for Rhodanese function and structure modulators. Some compounds are present in the metabolic pathway where Rhodanese is present. From the denaturation curves arising from DSF, melting temperatures can be extracted. That information can be compared between Rhodanese in "apo" form and the enzyme incubated with effectors.

The first DSF assays aimed to evaluate the effect of cysteine, thiosulfate, homocysteine and sulfite on Rhodanese stability.

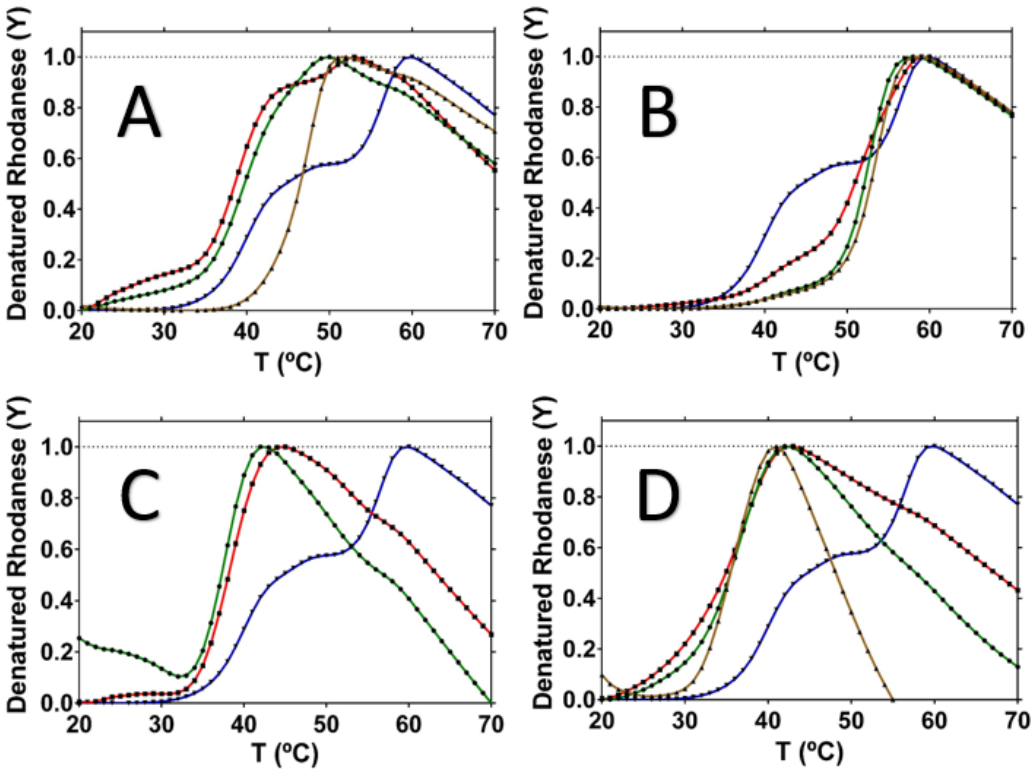

Figure 3.4 – DSF results with four different compounds. Panel A: Rhodanese with cysteine. Panel B: Rhodanese with thiosulfate. Panel C: Rhodanese with homocysteine. Panel D: Rhodanese with sulfite. Rhodanese "apo" data represented by blue curve. Rhodanese was pre-incubated with the compounds at 0.1 mM (red line), 1 mM (green) and 10mM (brown).

Globally, three effectors have similar results and the other one a totally different result. Studying separately, Rhodanese "apo" shows two different melting points, one at 40ºC and other at 55ºC, being fully denatured at 60ºC. When incubated with cysteine (Figure 3.4, Panel A), Rhodanese suffers destabilization since the denaturation temperature decreases, making it more thermolabile. Independently of effector concentration, cysteine yields a single melting transition, with a Tm around

40ºC, closer to Tm1, suggesting that cysteine affects the Rhodanese structure by destabilizing one of the two domains.

Thiosulfate has an opposite effect compared with cysteine, since it appears to stabilize Rhodanese (Figure 3.4, Panel B), making the enzyme more thermoresistant. The stabilizing effect affects the domain with the lower Tm, causing the protein to denature with a single transition closer to the 'Apo' Tm2. The fact that thiosulfate stabilizes Rhodanese may be related with fact that it is its reaction product.

Incubated with Rhodanese was also homocysteine (Figure 3.4, Panel C), a homologue of cysteine. Rhodanese suffers the same destabilization that cysteine caused. The melting point is only one, around 38ºC. Rhodanese in the presence of homocysteine gets completely denatured at a lower temperature, around 45ºC, a lower value compared with cysteine.

Sulfite results in the same destabilization behavior. Rhodanese incubated with sulfite (Figure 3.4, Panel D), is completely denatured at around 40ºC, with a single melting transition, with a Tm around 36ºC.

These results provided some useful information for the crystallization trials. Irrespectively of that, more compounds were tested to check the effects on the Rhodanese function. Some of them were selected with similar chemical structure to cysteine and others with proven effect on health [74]. The compounds tested were: S-allyl-cysteine (SAC), garlic oil, alliin and allyl sulfide.

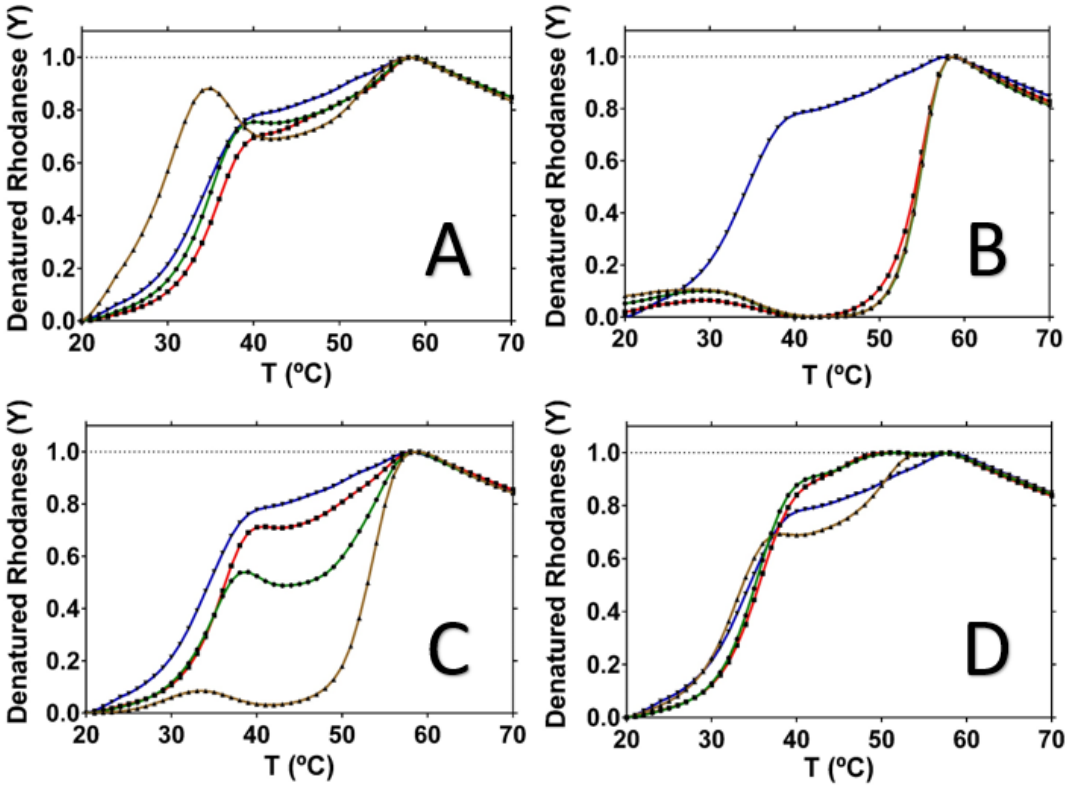

Figure 3.5 – DSF results with four different compounds. Panel A: Rhodanese with SAC. Panel B: Rhodanese with garlic oil. Panel C: Rhodanese with alliin. Panel D: Rhodanese with allyl sulfide. Rhodanese "apo" data represented by blue curve. Rhodanese was pre-incubated with the compounds at 0.1 mM or 0.001% (red line), 1 mM or 0.01% (green) and 10mM or 0.1% (brown).

Rhodanese "apo" data are different from the initial trials since the two melting transitions are not so well defined. The reason for that could be that the SYPRO [75] working concentration was wrong, since the commercial stock tends to degrade over time, which often results in an a priori protein destabilization. Nevertheless, and since DSF is essentially used as a comparative method, the effect of compounds can still be analyzed with respect to the 'Apo' data.

Regarding the SAC effect (Figure 3.5, Panel A), there are few changes compared to the normal behavior of Rhodanese. The denaturation of Rhodanese occurs at the same point independently of effector concentration. The only difference is in the highest effector concentration, 10mM, when the curve shows two different peaks and the melting points are affected. SAC is known to be a component of garlic extracts.

The effect of garlic oil on Rhodanese thermal denaturation (Figure 3.5, Panel B) is remarkable. It shows a stabilizing effect but more effective than thiosulfate in the first trials. Up until 50ºC, Rhodanese does not suffer any denaturation, then starts quickly and in a short break of temperature reaches the total denaturation. Also the results demonstrated a single melting transition, around 55ºC. Garlic oil consists of several components and it's interesting to see if each isolated

compound can do the same effect that this global effector [76]. As already demonstrated, SAC is not one of them.

Alliin, another garlic extract component (Figure 3.5, Panel C), has an identical effect. The effect is the same as the garlic oil but not so expressive. At lower concentrations (0.1mM and 1mM), Rhodanese still maintains two melting points. This effector has potential to induce some functional modifications on Rhodanese that could help the protein crystallization. Allyl sulfide (Figure 3.5, Panel D) had minor effects, despite being a garlic oil component. The effector concentration variation has influence on the stability of Rhodanese but not as much other effectors.

Table 3.1 – Melting points of Rhodanese in "apo" form and with several different effectors. n.t means "not tested". "---" represents the absence of results.

Effector	Concentration	Tm 1	Tm 2	Frac
Rhodanese "apo" 1		40ºC	55ºC	63%
Cysteine	0.1 mM	39ºC	---	---
	1 mM	40ºC	---	---
	10 mM	43ºC	---	---
Thiosulfate	0.1 mM	41ºC	51ºC	29%
	1 mM	43ºC	52ºC	15%
	10 mM	44ºC	53ºC	16%
Homocysteine	0.1 mM	38ºC	---	---
	1 mM	37ºC	---	---
Sulfite	0.1 mM	33ºC	---	---
	1 mM	36ºC	---	---
	10 mM	36ºC	---	---
Glutathione	0.1 mM	39ºC	---	---
	1 mM	39ºC	---	---
Rhodanese "apo" 2		33ºC	50ºC	86%
SMC	0.1 mM	35ºC	50ºC	80%
	1 mM	35ºC	52ºC	81%
	10 mM	34ºC	53ºC	77%
NAC	0.1 mM	---	---	---
	1 mM	39ºC	---	---
	10 mM	30ºC	---	---
SAC	0.1 mM	35ºC	51ºC	80%
	1 mM	34ºC	52ºC	82%
	10 mM	27ºC	53ºC	77%
Alliin	0.1 mM	35ºC	51ºC	77%
	1 mM	33ºC	52ºC	53%
	10 mM	28ºC	53ºC	5%
Garlic Oil	0.001%	---	55ºC	---
	0.01%	35ºC	54ºC	8%
	0.1%	35ºC	54ºC	9%

Allyl Sulfide	0.001%	35ºC	---	---
	0.01%	35ºC	47ºC	96%
	0.1%	32ºC	49ºC	73%

Taking into account the tested compounds, three effectors were selected to further study their effect on Rhodanese. Another method that can corroborate this data is a biophysical characterization by CD. If these results corroborate the DSF tests, all that information can be used for crystallization trials.

3.2.2 - Far-UV Circular Dichroism (CD) spectroscopy

The data provided by the DSF assays were important to select some compounds that modulate Rhodanese function [77]. To further evaluate the effect of these compounds, Far-UV circular dichroism was employed to study the effect of the compounds on the Rhodanese secondary structure.

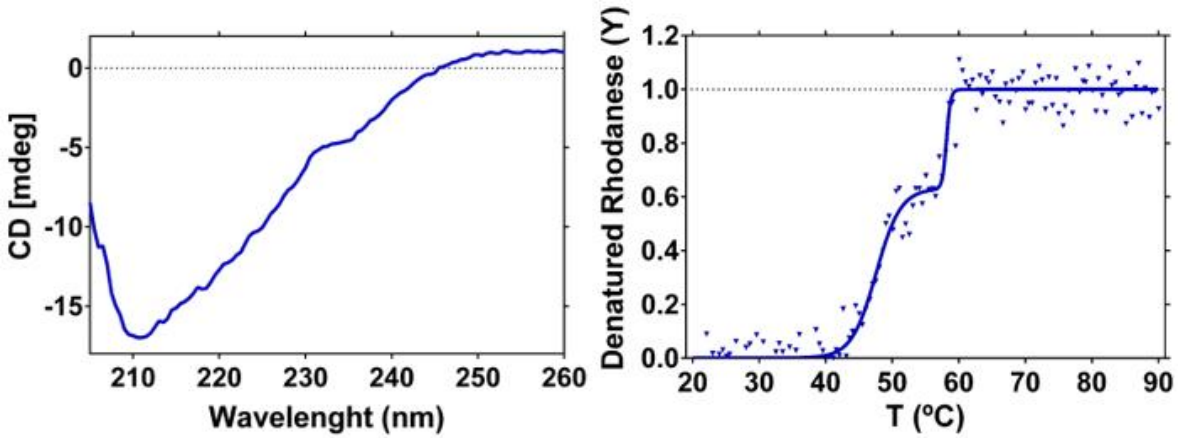

Figure 3.6 – On the left-panel, representation of a CD curve. On the right-panel, representation of a denaturation curve. The Rhodanese concentration is 0,26mg/mL. The CD experiment parameters were: Data pitch 0,5m. d.i.t 1 sec, scanning speed 50nm/min, band with 1nm. The denaturation curve was obtained with fixed wavelength of 222nm.

The denaturation curve (Figure 3.6, right-panel) corroborates the DSF curve of Rhodanese in "apo" form. There are two melting transitions, one with a Tm at 48ºC and another around 58ºC. The total denaturation occurs near 60ºC. The CD curve (Figure 3.6, left-panel) shows a decreasing curve with a minimum at 210nm of approximately -17 mdeg.

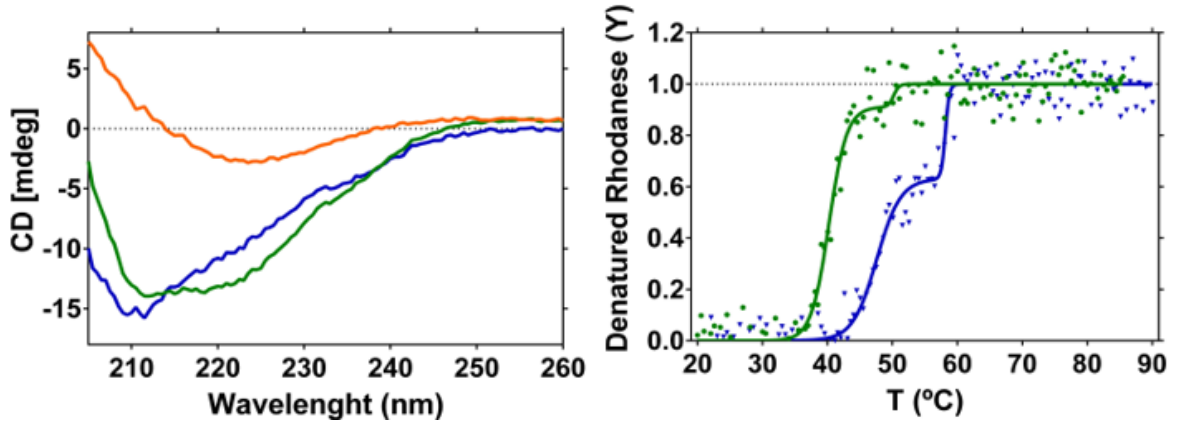

Figure 3.7 – On the left-panel, representation of a CD curve, where the orange line is cysteine ligand alone, the green line is the Rhodanese incubated with cysteine and the blue is the difference between the two curves. On the right-panel, representation of a denaturation curve, where in blue is Rhodanese in "apo" form and in green, Rhodanese incubated with cysteine. The Rhodanese final concentration is 0.26 mg/mL and the cysteine final

concentration is 1mM. The CD experience parameters were: Data pitch 0.5 m. d.i.t 1 sec, scanning speed 50nm/min, band with 1nm. The denaturation curve was obtained with fixed wavelength of 222nm.

Cysteine has a negligible effect on the spectral shape of Rhodanese, as compared to the isolated protein (Figures 3.6 and 3.7, left panel). Regarding the melting temperatures, cysteine causes a general decrease in thermal stability, with an 8ºC decrease in both Tm's, Rhodanese becoming totally denatured below 50ºC. This is the same effect that the DSF assay showed for cysteine.

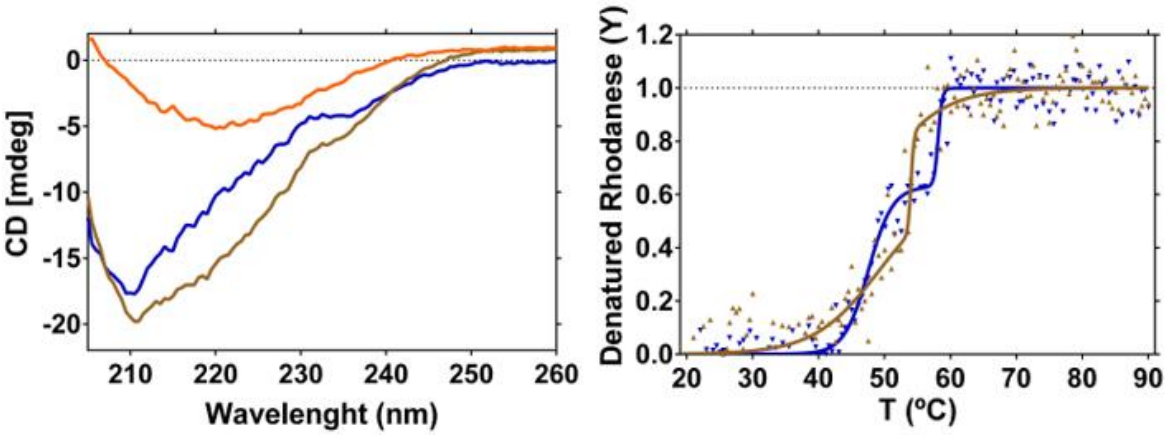

Figure 3.8 – On the left-panel, representation of a CD curve, where the orange line is thiosulfate ligand alone, the brown line is the Rhodanese incubated with thiosulfate and the blue is the difference between the two curves. On the right-panel, representation of a denaturation curve, where in blue is Rhodanese in "apo" form and in brown, Rhodanese incubated with thiosulfate. The Rhodanese final concentration is 0,26mg/mL and the thiosulfate final concentration is 1mM. The CD experience parameters were: Data pitch 0,5m. d.i.t 1 sec, scanning speed 50nm/min, band with 1nm. The denaturation curve was obtained with fixed wavelength of 222nm.

Like cysteine, thiosulfate had a negligible effect on the spectral features of Rhodanese. It is important to keep in mind that thiosulfate is the product of the reaction that Rhodanese catalyzes. The obtained Tm's, 49ºC and 54ºC, suggest a destabilization of the more stable domain (higher Tm) as compared to the 'Apo' enzyme, contrarily to the DSF results, where a stabilizing effect was shown.

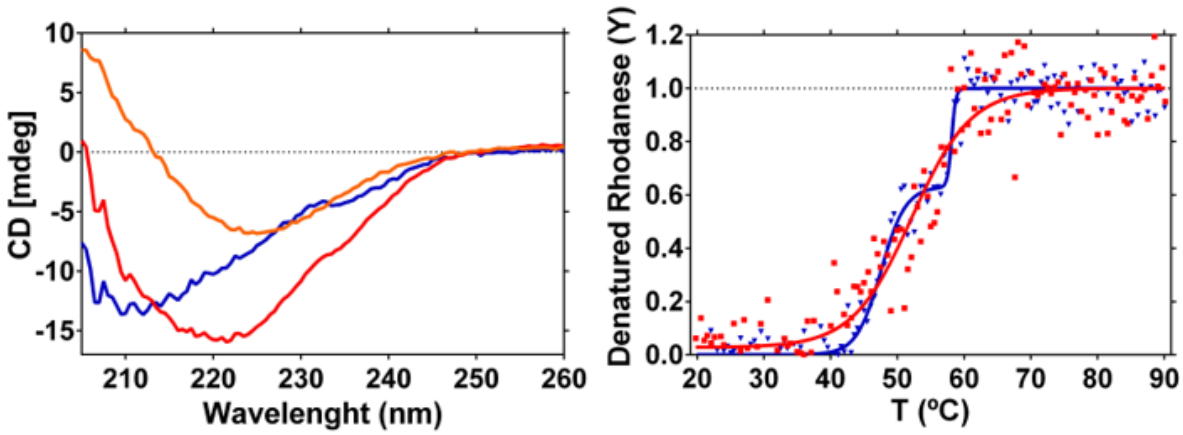

Figure 3.9 – On the left-panel, representation of a CD curve, where the orange line is alliin ligand alone, the red line is the Rhodanese incubated with thiosulfate and the blue is the difference between the two curves. On the right-panel, representation of a denaturation curve, where in blue is Rhodanese in "apo" form and in red, Rhodanese incubated with alliin. The Rhodanese final concentration is 0,26mg/mL and the alliin final concentration is 1mM. The CD experience parameters were: Data pitch 0,5m. d.i.t 1 sec, scanning speed 50nm/min, band with 1nm. The denaturation curve was obtained with fixed wavelength of 222nm.

Like the other two tested ligands, alliin also had practically null effects on the CD spectra of Rhodanese. In the CD-monitored experiments, alliin seems to alter the thermal denaturation profile without dramatically changing the thermal stability. Indeed, Rhodanese is denatured in a single transition, with a Tm of 53°C. These results also deviate from the DSF assays, although both methods indicate that alliin affects the overall Rhodanese stability.

Table 3.2 – Melting points of Rhodanese in "apo" form and incubated with three different ligands. The concentration values are the final concentration in the sample Rhodanese+Ligand. "---" represents the absence of results.

Effector	*Tm 1*	*Tm 2*
[Rhodanese]=0,26mg/mL	*48ºC*	*58ºC*
[Cysteine] = 1mM	*40ºC*	*50ºC*
[Thiosulfate] = 1mM	*49ºC*	*54ºC*
[Alliin] = 1mM	*53ºC*	---

Observing these values, it should be mentioned that altering the Rhodanese concentration but maintaining the ligand concentration results in slightly different Tm values. As a general conclusion, the CD assays corroborated the DSF trials in the sense that the chosen compounds affect the protein's thermal stability. Altogether, these data are a start point for crystallization trials in the presence of these compounds to check what effect they have in the global stability, conformation and function of the Rhodanese.

3.3 - Crystallization of Rhodanese

Successful purification of Rhodanese with high purity level made possible to proceed with initial crystallization trials to get Rhodanese crystals and determine its 3D crystallographic structure. The first screenings were with Rhodanese in its “apo” state at a concentration of 15 mg/mL using the commercially available screenings PACT Premier, JCSG+, SturaFootPrint and Structure Screen 1&2 (all from Molecular Dimensions). These plates were visualized for a long time but no crystals, or any other indication of possible crystal formation (crystalline material or spherulites) were observed. However, from the observations of the drops, one conclusion was that the protein concentration could be too high as inferred from the heavy precipitate observed in most drops.

The concentration of Rhodanese was then reduced to ~7,5 mg/mL and the crystallization screenings repeated as above. Since no crystals were still observed, we placed the hypothesis that Rhodanese could have difficulties to crystalize in its apo form. So, the next step was to use the information provided by CD and DSF. The three ligands with the more promising results on that trials, cysteine, thiosulfate and alliin, can cause some modification on Rhodanese and help crystallogenesis. In the sample preparation, Rhodanese was previously incubated with the ligands, separately. The final concentration of Rhodanese was 10mg/mL and the ligand concentration was 10mM. The screenings used were the same as before (Pact Premier, Structure Screen 1&2, JCSG+ and Footprint).

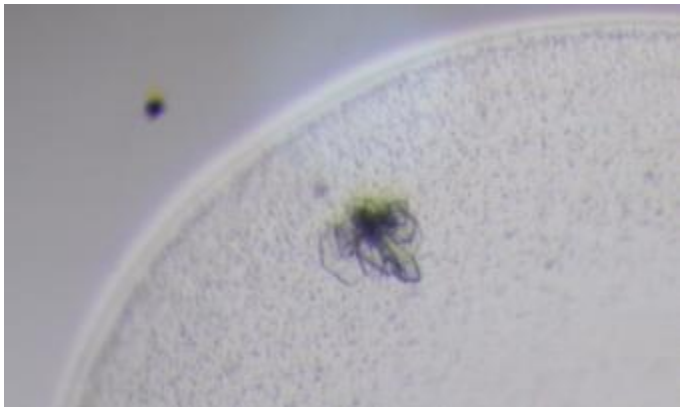

Figure 3.10 – Crystal photography of a hit in the Structure Screen 1&2 screening, taken with a Leica microscope coupled with a camera. The condition is Rhodanese in the presence of cysteine ligand.

Following this procedure, one hit from Rhodanese incubated with cysteine could be obtained in a drop comprising 0.05M potassium dihydrogen phosphate and 20%(w/v) PEG8000. This was the first result that could be used for testing and up-scaling. Data from this crystal was collected at beamline ID30A-1 of the ESRF (Grenoble – France) but as the diffraction pattern was typical of a salt crystal. At the same time, a scale up was done resulting is some crystal but later confirmed also as salt crystals. Until today, there were no developments with this cysteine ligand. The lack of results

forced us to employ a new strategy, like changing the screenings conditions. For that, the next trials were made with several other screenings, namely Midas, Morpheus, PGA and Clear Strategy, all based in non-PEG screenings, providing some complementary information. It is also adequate to soluble proteins. The Rhodanese concentration and ligand concentration remained the same. All this screening come out with no crystal formation.

So far, all these trials were made only with cysteine and thiosulfate ligands. Since there was a third promising ligand, alliin, we decided to do some screenings with that ligand. The firsts screenings with Rhodanese incubated with alliin were the ones used initially (Pact Premier, Structure Screen 1&2, JCSG+ and Footprint). The difference to the previous trials was that this one was made at the same ligand concentration (10mM) but with two different Rhodanese concentration (10 mg/ml and 5 mg/ml). So far, no crystals could be observed.

3.4 - Bio-SAXS of Rhodanese

For the SAXS experiments, the collected data were processed using programs from the *ATSAS* suite [60]. Data collection and reduction parameters are shown in Table 3.3. Three independent experiments were made: Rhodanese in its apo form, incubated with cysteine and incubated with thiosulfate. The I_0 represents the intensity when the scattering angle is zero, showing small differences between the three. The ligands themselves have a difference of 0.006 lower with thiosulfate, being thiosulfate the higher one. This could mean that Rhodanese is more dispersed on the solution. The radius-of-gyration (R_g), translates to the mass distribution of the molecule around its gravity center. Comparing the results, Rhodanse "apo" and Rhodanese incubated with thiosulfate have a very similar R_g, indicating that both are nicely compacted around the protein center of gravity. In case of cysteine presence, it seems to be not so compact.

One parameter that corroborates this statement is the D_{max} (nm), which gives information about the maximum distance between two appositive points (in a rough approximation, D_{max} can be translated to a diameter). The values of D_{max} indicated that Rhodanese incubated with cysteine is more elongated than with thiosulfate, where it seems more compact. This effect of cysteine corroborates the information of DSF and CD, making Rhodanese more labile to thermal denaturation. The same for thiosulfate, where the information of the biophysical methods show a Rhodanese more resistant to thermal denaturation.

Table 3.3 – SAXS data collection of Rhodanese and Rhodanese incubated with ligands cysteine and thiosulfate.

	"apo" Rhodanese	*Rhodanese + 1mM cysteine*	*Rhodanese + 1mM thiosulfate*
Primus Guinier Wizard			
I_0	0.0048 ± 1.7E-5	0.007 ±2.9E-5	0.013 ± 2.4E-5
R_g	2.06 ± 0.03	3.51 ± 0.37	2.13 ± 0.08
sR_g *limits*	0.50 ± 1.30	0.43 – 1.25	0.34 -1.29
Fidelity	0.85	0.94	0.95
Range	73 - 214	29 – 114	42 – 205
Distance distribution (GNOM)			
D_{max}*(nm)*	6.42 (64.2*Å)*	6.80 (68*Å)*	6.29 (62.9*Å)*
Quality	65.03	61.94	62.84
Range	73 – 1200	210 – 1300	150 – 1349
Real space I_0	0.00473	0.00401	0.01237
Real space R_g	2.042	2.266	2.026
Reciprocal space I_0	0.00473	0.00401	0.01237
Reciprocal space R_g	2.041	2.261	2.026
Dammin (default settings)			
Chi^2	1.120	2.285	1.250

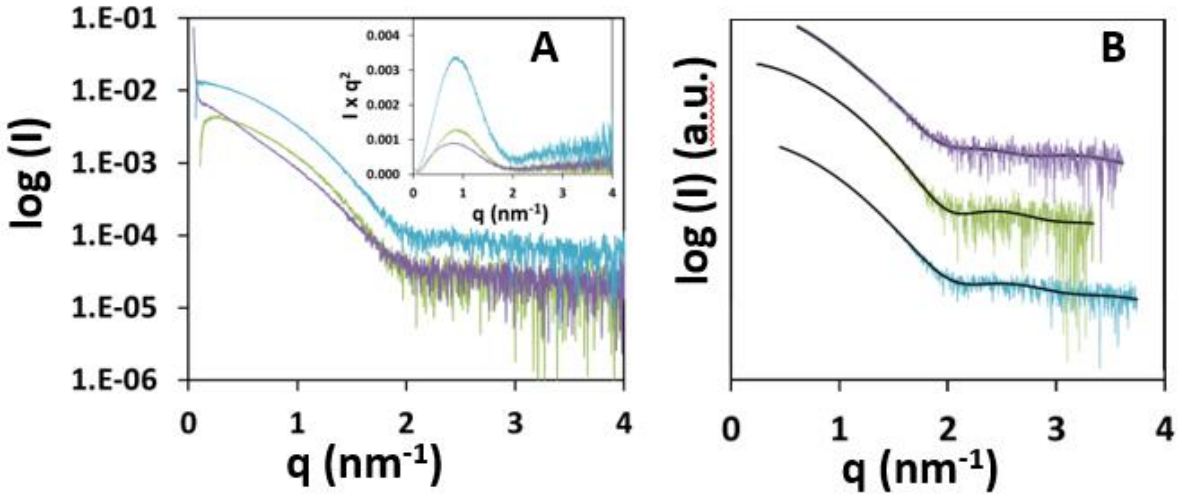

Figure 3.11 – SAXS analysis of human Rhodanese. On the panel A, raw SAXS curves recorded in the "apo" form (green) or presence of cysteine (purple) and thiosulfate (blue). Inset, corresponding Kratky plot (with same color code). The panel B, are the fitted curves (parameters in the Table 3.3).

The raw curves of Rhodanese "apo" and with ligands, (Figure 3.11, panel A), confirms that Rhodanese is properly folded presenting a globular shape (also confirmed by the Kratky plot). However, the curves also suggest that the protein adopts different conformations in solution. Rhodanese incubated with thiosulfate seems to have the more compact folding.

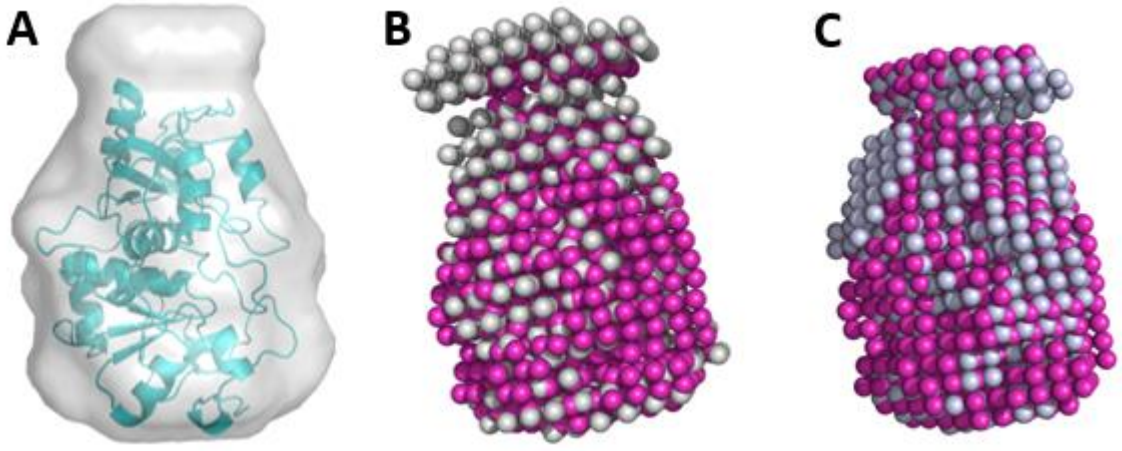

Figure 3.12 – SAXS structural models of human Rhodanese. Panel A, molecular shape of "apo" human Rhodanese (blue carton representation corresponds to 3D model based on the bovine Rhodanese structure, PDB code: 1boh). Panel B, bead models of human Rhodanese in the absence (magenta) or presence of cysteine (green). Panel C, bead models of human Rhodanese in the absence (magenta) or presence of thiosulfate (blue).

The model of Rhodanese generated by SWISS-MODEL (Figure 1.6) seems to fit well with the SAXS data of Rhodanese "apo" (Figure 3.12, A), where it can be seen an unfilled region near the N-terminal terminus, where is located the His-tag and the PreScission cutting peptide. Like the data

analyzed before, the ligand models (Figure 3.12, B and C), show the same conformation. Cysteine assumes a more elongated form and thiosulfate a more compact.

Overall, the low resolution models support the biophysical characterization of the ligands effect on the protein thermal stability. Together with DSF and CD data, these two ligands have practical conditions to be used in crystallization trials since both appear to affect the protein structure.

3.5 - Model Building of CBS

The mutation P49L, although not one of the most frequent, can be a source to classical homocystinuria. Crystallization and structure determination of this variant of CBS could help to understand some modifications on the structure by comparison to the wild type structure. The mutation P49L is observed in all chains of CBS (Figure 3.13). This is not surprising since the presence of the mutation was already verified in the gene expression step and activity assays. The construct used for crystallization has 408 amino acids. However, some loop regions are not observed in all six chains.

Noteworthy, these loop regions are also disordered in the published structure (1JBQ). Remarkable, the fact that in our model was possible to model some region that are absent for the wt CBS also worked on this project (data not shown; refinement under progress). Regarding those loop regions, loop 193-202 located in a cleft that leads from the solvent to the PLP moiety, in CBS P49L, in one chain (chain D) has the loop all built. Comparing that region with a published wild type (PDB code: 1JBQ), it seems to be a more defined loop and with less flexible. In the complete structure (not the truncated form used in the present study), this loop is stabilized by the C-terminus. It is not possible to confirm if it is the P49L mutation that causes this change but it seems to be more of a question of crystal packing that helps stabilization of the loop.

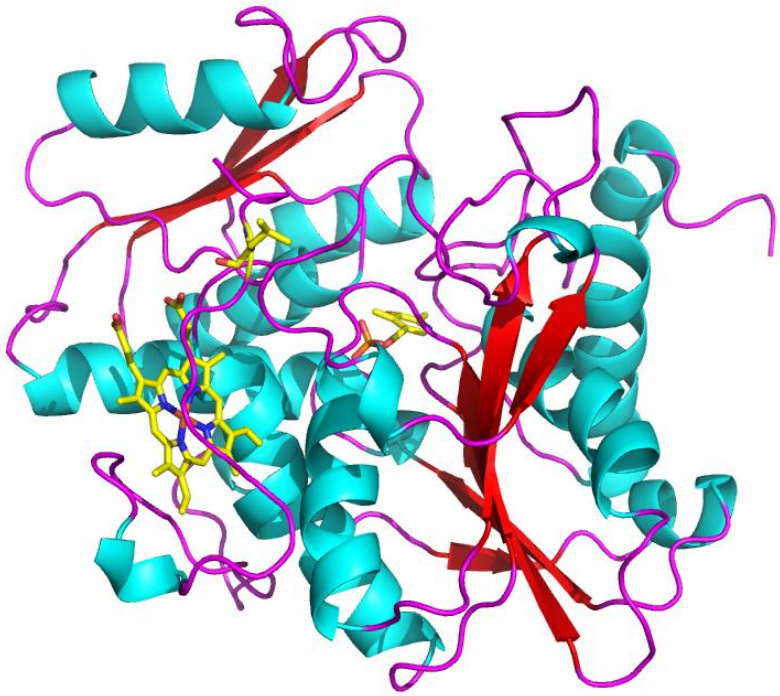

Figure 3.13 – Cartoon representation of mutant CBS P49L, highlighting the heme group, the PLP co-factor and the residue 49 (local of the mutation).

Comparing the P49L structure reported herein with the previously published structure (Figure 3.14), it can be seen that the PLP moiety does not suffer any changes regarding its binding site. The same is true for the heme moiety. However, the less flexible leucine residue introduced with the mutation seems to alter the loop flexibility making it more rigid.

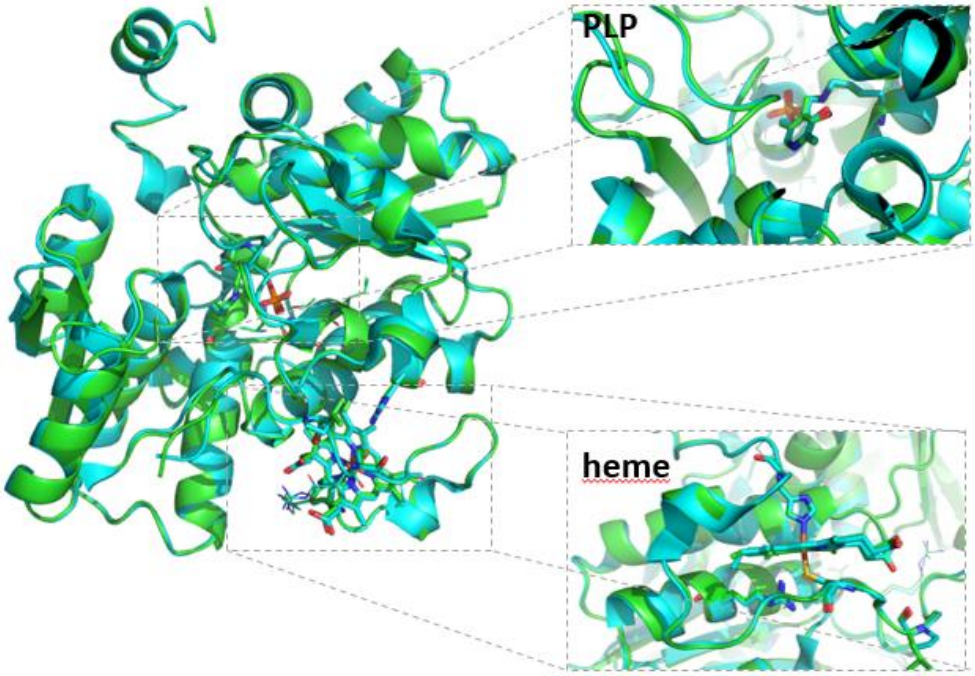

Figure 3.14 – Cartoon representing the superimpose of mutant CBS P49L with a published structure, with the PDB code: 1JBQ [78]

3.6 - Expression and Purification of SQR

SQR is a membrane protein so it requires different expression and purification methods [79]. As Rhodanese, reported expression protocol in *Lybiad et.all* [27] was used. The production has begun with 8L from which 56g of cell mass were obtained and then cell lysis done by French press. After the expression, the step of purification started with an affinity exchange column, since the SQR plasmid was built with the presence of a His-Tag. For pursing this purification, it was necessary to stabilize the protein since his membrane-bound proprieties. For that stabilization, was used glycerol and one detergent, in this case, Triton X-100 [80].

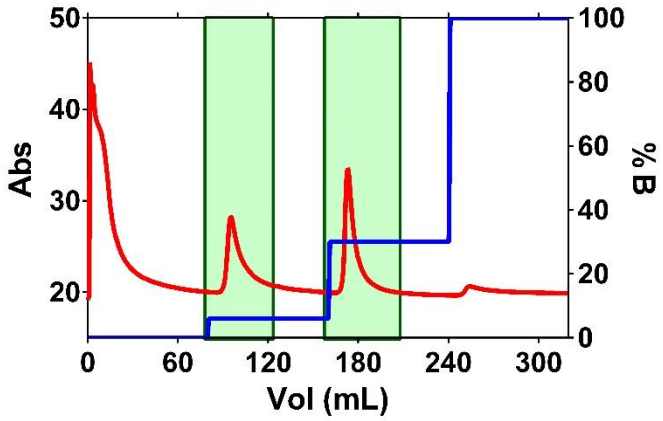

Figure 3.15 – Chromatogram of SQR affinity chromatography. Purification conditions were: Flow 2mL/min, 2mL for fraction. Two step gradients at 6% and 30%. Fractions in the green box were collected. Used column with a total volume of 5mL. 50x downscale.

Previous tests of this purification suggested two possible values of binding buffer where SQR elutes, one at 6% (30mM Imidazole) and the other one at 30% (150mM Imidazole) of binding buffer. Two different fractions were collected and the presence of SQR was checked by SDS-PAGE (Appendix 4) and Western Blot (Appendix 5). The fraction of 6% is considered Fraction A and the fraction of 30% is considered Fraction B.

Another important step is to remove the imidazole present because it will interfere with the global stability of SQR. The next step is an anionic chromatography (containing positive charge that will retain the negative elements). By having two different fractions, it was necessary to do the next purification steps twice.

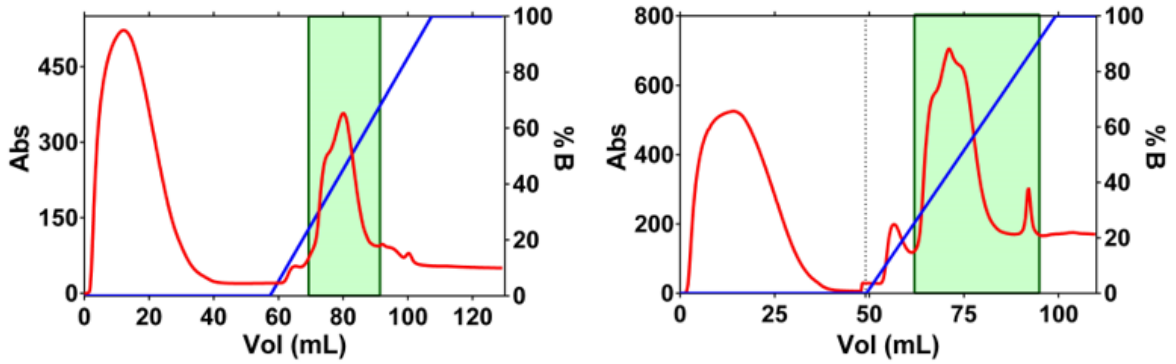

Figure 3.16 – Chromatogram of SQR anionic exchange chromatography. In the left panel the chromatogram of Fraction A and on the right panel the chromatogram of Fraction B. Purification conditions were: Flow 2mL/min, 4mL for fraction. Fractions in the green box were collected. Used column with a total volume of 5mL. In the chromatogram of the right, upscale when gradient start 5x.

Both fractions have revealed similar results, with a little exception on the Fraction B, where are two different peaks. For that reason, all the fractions in the green box were pooled and collected to be analyzed by SDS-PAGE (Appendix 6), and Western Blot (Appendix 7). The fraction on the right is designated as Fraction B1 and the one on the left by Fraction A1. The results show the presence of SQR but with many contaminants. At this stage, already the low yield of SQR can be observed.

So far, all the purification steps were occurring with positive results, all confirmed by the SDS-PAGE and Western blot analyses. The same method proved that the SQR was not totally pure so it was necessary to do another purification step to increase the purity. The third method was a molecular exclusion chromatography.

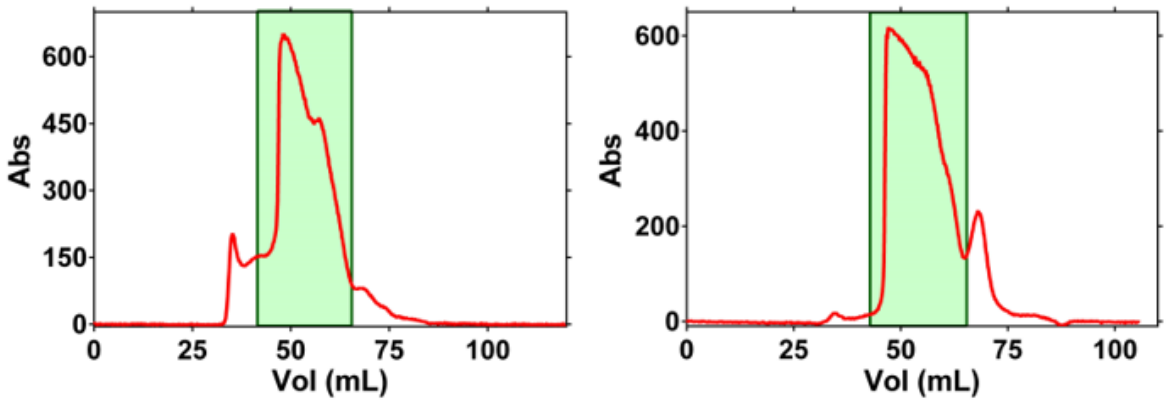

Figure 3.17 – Chromatograms of SQR molecular exclusion chromatography. In the left panel the chromatogram of Fraction A1 and on the right panel the chromatogram of Fraction B1. Purification conditions were: Flow 0,6mL/min, 1,5mL for fraction. Fractions in the green box were collected. Used column with a total volume of 120mL.

The fraction collected on the left purification was nominated by Fraction A1A and the one on the right purification is nominated Fraction B1B. Both fractions were analyzed by SDS-PAGE (Appendix 8) and Western Blot (Appendix 9). The results show the presence of SQR but far away from a pure state. In this state, the protocol by *Lybiad et.all* was already done and the SQR was not pure as the authors reported. Gathering this information, another purification step was required, making another anion exchange chromatography using a ResourceQ. This type of column is more specific than the HiTrap columns used before. This time, only one fraction was purified, the Fraction B1B.

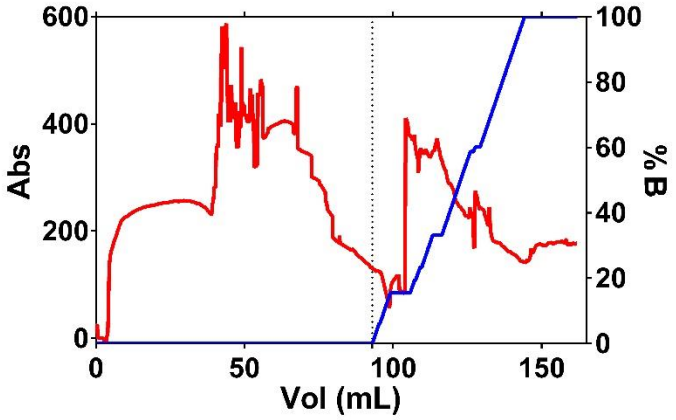

Figure 3.18 – Chromatograms of SQR ResourceQ chromatography. Purification conditions were: Flow 1mL/min, 1mL for fraction. Used column with a total volume of 5mL. Dotted line represent the start of the gradient, that is upscale 5x.

Global result was far from expected. The technique was to use a linear gradient with steps in areas when the reading absorbance had a tendency to increase. The fractions that containing that absorbance increase, were collected and characterized by SDS-PAGE (Appendix 10), and Western Blot (Appendix 11), with some interesting results. Besides the behavior of the chromatogram, that can be explained by an interfering detector, the biophysical methods show the presence of vestigial SQR with a good purity.

It is known that SQR have a low production field but with higher purity grade. In this case, it was not possible to get significate amount. Besides the protocol was followed to the letter, the final result wasn't the same. The reason that can explain that is the SQR was not comfortable with some steps of freeze/unfreeze during the process. Another explanation was some different reagents used instead of the designate in protocol. The final conclusion is that SQR is like the other membrane-proteins, very sensitive to purification methods and is necessary to have a regular process and having control of all the variables of the process.

4 – Conclusions and Future Work

Rhodanese purification resulted in a yield of 2mg of protein per Liter of culture media. This yield allowed us to produce enough protein for the different structural studies and biophysical methods employed in this study. Although we did not manage to get crystals of Rhod, it was possible to understand how the structure can be affected in the presence of certain modulators. Studies of DSF, CD and SAXS show that cysteine, thiosulfate and alliin have different effects on the Rhodanese structure, namely stabilizing or disturbing it. To understand more deeply the behavior of this protein, some additional experience is needed to see with other effectors can modify is function and if it helps to crystal formation.

SQR purification shows a protein very sensitive to conditions variation and, besides some results, far from the ideal. Further studies, like more steps of protein stabilization or without resorting any freezing step, are necessary to understand how the protein can be stabilized. The purification of SQR, if successful, can lead to some biochemical studies and to crystallization trials.

CBS model building of the mutation P49L shows that this classical homocystinuria mutation does not have a major impact on the overall fold of CBS, since very few changes, namely on active site distant loops, could be observed but more likely to be caused by crystal packing that helps stabilize the loop. Working on the WT-CBS can help to understand more about some modification in relation with P49L. Another interesting experience passes by introduction of a ligand in the CBS crystal by co-crystallization to see the modification on the structure.

5 – References

[1] – Fred N. Tebbe et all. Composition of elemental sulfur in solution: equilibrium of S6,S7 and S8 at ambient temperatures. J.Am.Chem.Soc 1982, pp 4971-4972.

[2] – M.E. Wieser and T.B. Coplen. Pure appl. Chem. 2011, pp 359-396 @ International Union of Pure and Applied Chemistry (IUPAC)

[3] – "Sulfur (revised)". Chemical Elements: From Carbon to Krypton, The Gale Group, 2006

[4] – Parcell S. Sulfur in human nutrition and applications in medicine. Altern.Med.Rev, 2002, pp 22-44.

[5] – M.J. Bickle et all. Sulphur transport and Sulphur isotope fractionations in ocean floor hydrothermal systems. Mineralogical Magazine, Volume58A, pp-88-89

[6] – Grimble RF. The effects of sulfur amino acid intake on immune functions in humans. Journal Nutrition, 2006, pp 1660-1665

[7] – Jorgensen BB. A thiosulfate shunt in the sulfur cycle of marine sediments. Science. 1990, pp 152-154

[8] – Wang XB et all. The biological effect of endogenous sulfur dioxide in the cardiovascular system. Journal Pharmacol, 2011, pp 1-6

[9] – K.Ono et all. Redox chemistry and chemical biology of H2S, hydropersulfides, and derived species: implications of ther possible biological activity and utility. Biol. Med Vol 77. 2014, pp 82-94

[10] – Yaqian Huang et all. Endogenous Sulfur Dioxide: A new member of Gasotransmitter Family in the Cardiovascular System. Oxidative Medicine and Cellular Longevity, 2016

[11] – S.Ramasamy et all. Sulfide-detoxifying enzymes in the human colon are decreased in cancer and upregulated in differentiation. American Physiological Society, 2006, pp 288-296

[12] – Miller AL et all. The methionine-homocysteine cycle and its effects on cognitive diseases. Altern.Medical.Review, 2003, pp 7-19

[13] – Rey FE et all. Metabolic niche of a prominent sulfate-reducing human gut bacterium. Academy Sci USA, 2013

[14] – Franck Carbonero et all. Microbial pathways in colonic sulfur metabolism and links with health and disease. Front. Physiol. 2012, pp 448

[15] – Henk J. Blom et all. Overview of homocysteine and folate metabolism. With special references to cardiovascular disease and neural tube defects. Journal Inherit.Metab.Dis, 2011, pp 75-81

[16] – Vicente JB et all. Bioenergetic relevance of hydrogen sulfide and the interplay between gasotransmitters at human cystathionine β-synthase. Biochimica et Biophysica Acta, 2016

[17] – Sun Q. et all. Structural basis for the inhibition mechanism of human cystathionine gamma-lyase, and enzyme responsible for the production of H(2)S. Journal Biol.Chem. 2009, pp-3076-3085

[18] – Jiang X et all. Expression, purification and preliminary crystallographic studies of human glutamate oxaloacetate transaminase 1 (GOT1). Protein Expression Purification, 2015

[19] – Chiku T et all. H2S biogenesis by human cystathionine gamma-lyase leads to the novel sulfur metabolites lanthionine and homolanthionine and is responsive to the grade of hyperhomocysteinemia. Journal Biol.Chem. 2009, pp 11601-11612

[20] – Miyamoto R et all. Contribution of cysteine aminotransferase and mercaptopyruvate sulfurtransferase to hydrogen sulfide production in peripheral neurons. Journal Neurochemistry, 2014, pp 29-40

[21] – Pramod Kumar Yadav et all. Structure and Kinetic Analysis of H2S Production by Human Mercaptopyruvate Sulfurtransferase. Journal Biol.Chem Vol.288. 2013, pp 2002-20013

[22] – Andreas Papapetropoulos et all. Pharmacology of the 'gasotransmitter' NO, CO and H2S: translational opportunities. Journal Pharmacol. 2015, pp 1395-1396

[23] – Abbas Abou-Hamdan et all. Positive feedback during sulfide oxidation fine-tunes cellular affinity for oxygen. Biochimica et Biophysica, 2016, pp 1464-1472

[24] – Tatiana V. Mishanina et all. Transient Kinetic Analysis of Hydrogen Sulfide oxidation catalyzed by Human Sulfide Quinone Oxidoreductase. JBC paper, 2015

[25] – Frédéric Bouillaud et all. Mitochondria and Sulfide: A very old story of poisoning, feeding and signaling. Antioxidants & Redox Signaling Vol.15. 2011, pp 379-391

[26] – Pettianati I. et all. Crystal structure of human persulfide dioxygenase: structural basis of ethylmalonic encephalopathy. Hum.Mol.Genet. 2015, pp 2458-2469

[27] – Libiad M. et all. Organization of the human mitochondrial hydrogen sulfide oxidation pathway. Journal Biol.Chem., 2014

[28] – Alexandre Smirnov et all. Mitochondrial Enzyme Rhodanese Is Essential for 5S Ribosomal RNA import into Human Mitochondria. Journal Biological Chemistry Vol.285. 2010, pp 30792-30803

[29] – R.Picton et all. Mucosal protection against sulphide: importance of the enzyme Rhodanese. Gut. 2002 Feb; 50(2): 201–205

[30] – Wang J. et all. Sulfite oxidase catalyzes Single-Electron transfer at Molybdenum domain to reduce nitrite to nitric oxide. Antioxid. Redox Signal. 2015, pp 283-94

[31] – Mendes MI. et all. Insights into the regulatory domain of cystathionine Beta-synthase: caractherization of six variant proteins. Hum.Mutat. 2014, pp 1195-1202

[32] – June Ereño-Orbea et all. Structural insight into the molecular mechanism of allosteric activation of human cystathionine β-synthase by S-adenosylmethionine. PNAS. 2014, pp 3845-3852

[33] – June Ereño-Orbea et all. Structural basis of regulation and oligomerization of human cystathionine β-synthase, the central enzyme of transsulfuration. PNAS. 2013, pp 3790-3799

[34] – Szabó C. Hydrogen sulphide and its therapeutic potencial. Nat.Rev.Drug.Discov. 2007, pp 917-935

[35] – Marisa I.S. Mendes et all. Reduced response of Cystathionine Beta-Synthase (CBS) to S-Adenosylmethionine (SAM): Identification and functional analysis of CBS gene mutations in Homocystinuria patients. Journal of Inherited Metabolic Disease Vol.37. 2014, pp 245-254

[36] – Jonathan D. Picker et all. Homocystinuria caused by Cystathionine Beta-Synthase deficiency. GeneReviews. 2014

[37] – Ales Hnízda et all. Conformational proprieties of nine purified cystathionine beta-synthase mutants. Biochemistry. 2012, pp 4755-4763

[38] – Omer Kabil et all. Enzymology of H_2S Biogenesis, Decay and Signaling. Antioxid.Redox.Signal. 2014, pp 770-782

[39] – Vicente JB. et all. S-Adenosyl-l-methionine Modulates CO and NO Binding to the Human H2S-generating Enzyme Cystathionine β-synthase. Journal Biol.Chem. 2016, pp 572-581

[40] – M. Ackermann et all. The vertebrate homologue of sulfide-quinone reductase in mammalian mitochondria. Cell Tissue. 2014, pp 779-792

[41] – Jackson MR. et all. Human sulfide:quinone oxidoreductase catalyzes the first step in hydrogen sulfide metabolism and produces a sulfane sulfur metabolite. Biochemistry. 2012, pp 6804-6815

[42] – Brito, J.A. et all. Structural and functional insights into sulfide:quinone oxidoreductase. (2009) Biochemistry 48: 5613-5622

[43] – Maia M. Cherney et all. Structure-activity characterization of sulfide:quinone oxidoreductase variants. Journal of Structural Biology Vol.178. 2012, pp 319-328

[44] – Leung P.. et all. Encapsulation of thiosulfate: cyanide sulfurtransferase by mouse erythrocytes. Toxicol App. Pharmacol. 1986, pp 101-107

[45] – Marouane Libiad et all. Polymorphic variants of Human Rhodanese exhibit differences in thermal stability and sulfur transfer kinetics. Journal Biological Chemistry Vol.290. 2015, pp 23579-23588

[46] – Trevino, R.J et all. NH2-terminal sequence truncation decreases the stability of bovine Rhodanese, minimally perturbs its crystal structure, and enhances interactions with GroEL under native conditions. J.Biol.Chem Vol.274. 1999, pp 13938-13947

[47] – Marco Biasini, Stefan Bienert, Andrew Waterhouse, Konstantin Arnold, Gabriel Studer, Tobias Schmidt, Florian Kiefer, Tiziano Gallo Cassarino, Martino Bertoni, Lorenza Bordoli, Torsten Schwede. (2014). SWISS-MODEL: modelling protein tertiary and quaternary structure using evolutionary information. *Nucleic Acids Research*; (1 July 2014)

[48] – Kiefer F, Arnold K, Künzli M, Bordoli L, Schwede T (2009). The SWISS-MODEL Repository and associated resources. *Nucleic Acids Research*. 37, D387-D392.

[49] – Guex, N., Peitsch, M.C., Schwede, T. (2009). Automated comparative protein structure modeling with SWISS-MODEL and Swiss-PdbViewer: A historical perspective.*Electrophoresis*, 30(S1), S162-S173

[50] – Arnold K., Bordoli L., Kopp J., and Schwede T. (2006). The SWISS-MODEL Workspace: A web-based environment for protein structure homology modelling. *Bioinformatics*, 22,195-201.

[51] – Mei-Chu Lo et all. Evaluation of fluorescence-based thermal shift assay for hit identification in drug discovery. Analytical Biochemistry Vol.332. 2004, pp 153-159

[52] – Steinberg TH et all. Applications of SYPRO orange and SYPRO red proteins gel stains. Anal. Biochemistry. 1996, pp 238-45

[53] – Norma J. Greenfield. Using circular dichroism spectra to estimate protein secondary structure. Nat. Protoc. 2009

[54] – Sharon M. Kelly et all. How to study proteins by circular dichroism. Biochimica et Biophysica. 2005, pp 119-139

[55] - Dessau MA et all. Protein crystallization for X-ray crystallography. J Vis Exp. 2011 Jan 16;(47). pii: 2285

[56] - Wlodawer A et all. Protein crystallography for non-crystallographers, or how to get the best (but not more) from published macromolecular structures. FEBS J. 2008. 275,1-21

[57] - Practical Approaches to Biological Inorganic Chemistry. Chapter 9 X-ray Crystallography Jose´ A. Brito and Margarida Archer Membrane Protein Crystallography Laboratory, ITQB

[58] - Ilari A et all. Protein structure determination by x-ray crystallography. Methods Mol Biol. 2008;452:63-87

[59] – Alexey G. Kikhney et all. A practical guide to small angle X-ray scattering (SAXS) of flexible and intrinsically disordered proteins. FEBS Vol.589. 2015, pp 2570-2577

[60] - Petoukhov, M.V., Franke, D., Shkumatov, A.V., Tria, G., Kikhney, A.G., Gajda, M., Gorba, C., Mertens, H.D.T., Konarev, P.V. and Svergun, D.I.*J. Appl. Cryst.* 45. 2012, pp 342-350

[61] - D. I. Svergun (1999) Restoring low resolution structure of biological macromolecules from solution scattering using simulated annealing. *Biophys J.* 2879-2886.

[62] - Wolfgang Kabsch, XDS. Acta Crystallogr D Biol Crystallogr. 2010 Feb 1; 66(Pt 2): 125–132.

[63] - P.R.Evans "An introduction to data reduction: space-group determination, scaling and intensity statistics", Acta Cryst. D67, 282-292 (2011)

[64] - P.R. Evans and ,G.N. Murshudov "How good are my data and what is the resolution?" Acta Cryst. (2013). D69, 1204–1214

[65] - Vonrhein C. Data processing and analyses with the autoPROC toolbox. Acta Crystallogr D Biol Crystallogr. 2011 Apr;67(Pt 4):293-302

[66] - Blanc E, Roversi P, Vonrhein C, Flensburg C, Lea SM, Bricogne G. (2004). Refinement of severely incomplete structures with maximum likelihood in BUSTER-TNT. Acta Crystallogr D60, 2210-21

[67] - Paul Emsley and Bernhard Lohkamp and William G. Scott and Kevin Cowtan},{Features and Development of Coot. Acta Crystallographica Section D - Biological Crystallography},2010,66,486-501

[68] – Germán L.Rosano et all. Recombinant protein expression in Escherichia coli: advances and challenges. Front microbial. 2014, pp 172

[69] - Josefine Ederth et all. A single-step method for purification of active His-tagged ribosomes from a genetically engineered Escherichia coli. Nucleic Acids Res. 2009 Feb

[70] – Structure Genomins consortium et all. Protein production and purification. Nat. Methods V5. 2011, pp 369

[71] - Paula Hong et all. Size-Exclusion Chromatography for the Analysis of Protein Biotherapeutics and their Aggregates. J Liq Chromatogr Relat Technol. 2012 Nov; 35(20): 2923–2950

[72] - Cummins PM et all. Ion-exchange chromatography: basic principles and application to the partial purification of soluble mammalian prolyl oligopeptidase. Methods Mol Biol. 2011;681:215-28

[73] – Carlsson N et all. Quantification of protein concentration by the Bradford method in the presence of pharmaceutical polymers. Anal.Biochem. 2011, pp 116-121

[74] – Sheen LY et all. Effects of garlic oil and its organosulfur compounds on the activities of hepatic drug-metabolizing and antioxidant enzymes in rats fed high- and low-fat diets. Nutr. Cancer. 1999, pp 160-166

[75] – Morten K. Groftehauge et all. Protein-Ligand interactions investigated by thermal shift assay (TSA) and dual polarization interferometry (DPI). Acta Crystallographic D. 2015, pp 36-44

[76] – E.A.O'Gara et all. Activities of garlic oil, garlic powder, and their diallyl constituents against *Helicobacter pylori*. Appl. Enviro. Microbiol. 2000, pp 2269-2273

[77] – Norma J. Greenfield. Using circular dichroism collected as a function of temperature to determine the thermodynamics of protein unfolding and binding interactions. Nat. Protoc. 2009

[78] – Meier, M. et all. Structure of human cystathionine beta-synthase: a unique pyridoxal 5'-phosphate-dependent heme protein. 2001. EMBO J. 20: 3910-3916

[79] – Smith SM. Strategies for the purification of membrane proteins. Methods Mol Biol. 2011, pp 485-496

[80] – Lin SH. Purification of membrane proteins. Methods Enzimol. 2009, pp 619-629

6 – Appendix

6.1 – Appendix 1: SDS-PAGE analyze of Rhodanese affinity chromatography

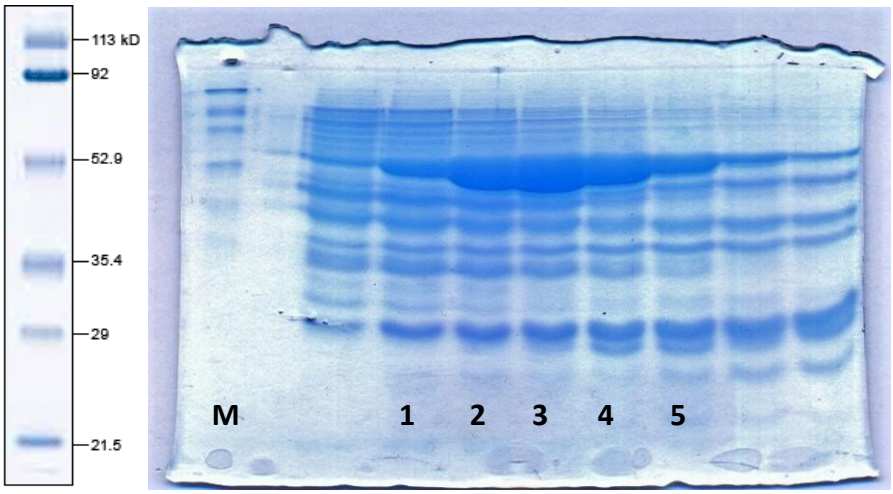

Figure 6.1 – Fractions collected from this chromatography. Fractions 1-5 pooled and concentrated for the next purification step. Marker "M" SDS-PAGE Standards, low range.

6.2 – Appendix 2: SDS-PAGE analyze of Rhodanese molecular exclusion chromatography

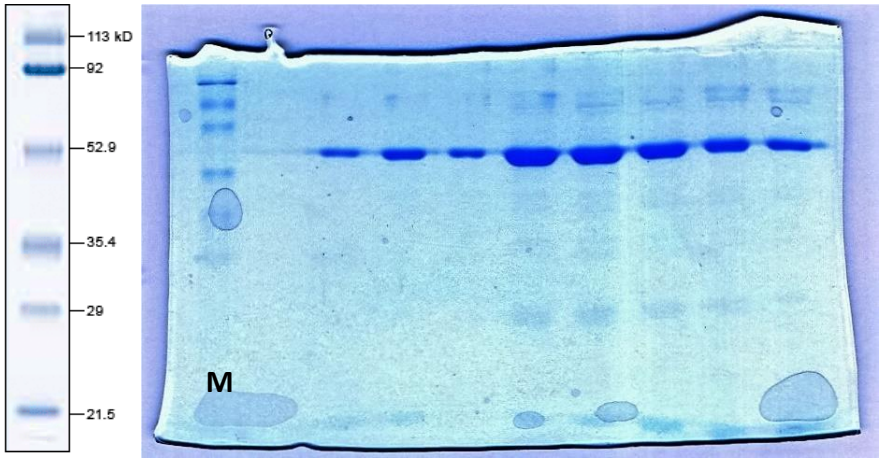

Figure 6.2 – Fractions collected from this chromatography. All this Fractions pooled and concentrated for the next purification step. Marker "M" SDS-PAGE Standards, low range.

6.3 – Appendix 3: SDS-PAGE analyze of Rhodanese anionic exchange chromatography

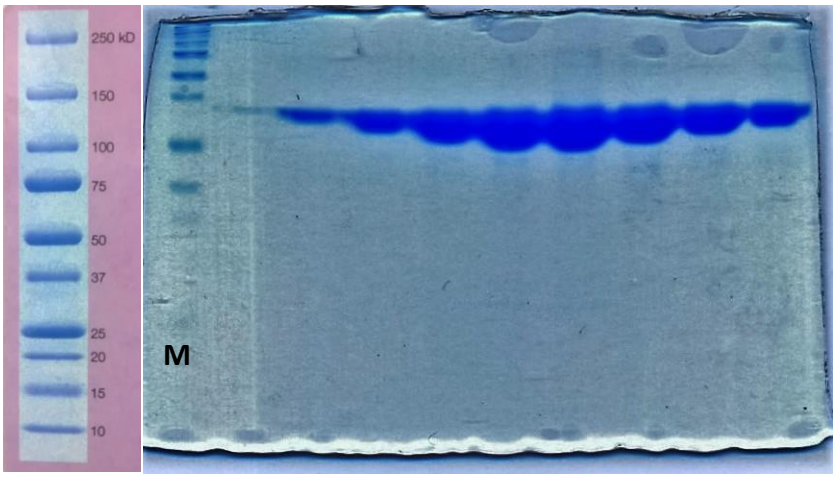

Figure 6.3 - Fractions collected from this chromatography. All this Fractions pooled and concentrated for protein concentration determination. step Marker "M" Precision Plus Protein Standards (BioRad).

6.4 – Appendix 4: SDS-PAGE analyze of SQR affinity chromatography

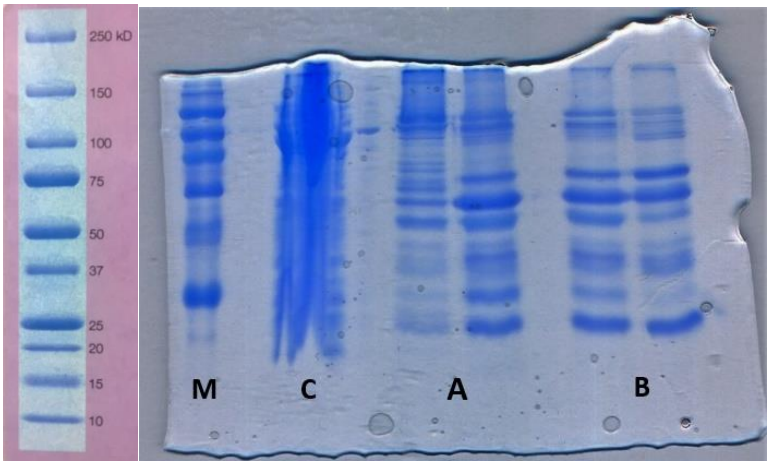

Figure 6.4 – Fraction "A" corresponds to 6% binding buffer and Fraction "B" to 30% binding buffer. "C" represents the sample that was loaded on the column. Marker "M" Precision Plus Protein Standards (BioRad).

6.5 – Appendix 5: Western Blot analyze of SQR affinity chromatography

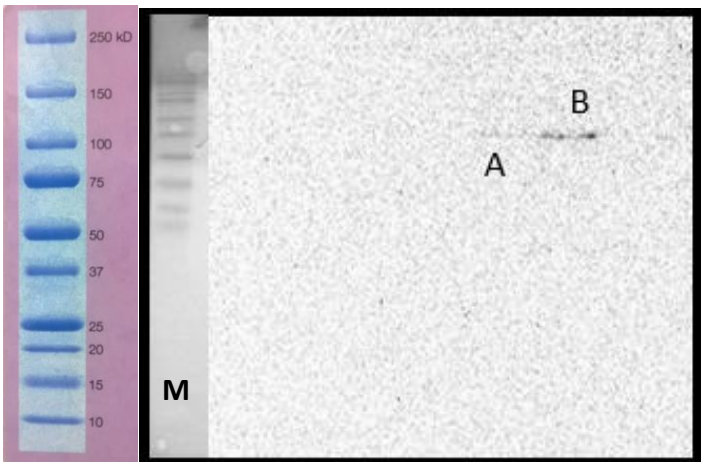

Figure 6.5 – Fraction "A" corresponds to 6% binding buffer (denominated Fraction A) and Fraction "B" to 30% binding buffer (denominated Fraction B). Marker "M" Precision Plus Protein Standards (BioRad). WB done with anti-SQR antibody.

6.6 – Appendix 6: SDS-PAGE analyze of SQR anionic exchange chromatography

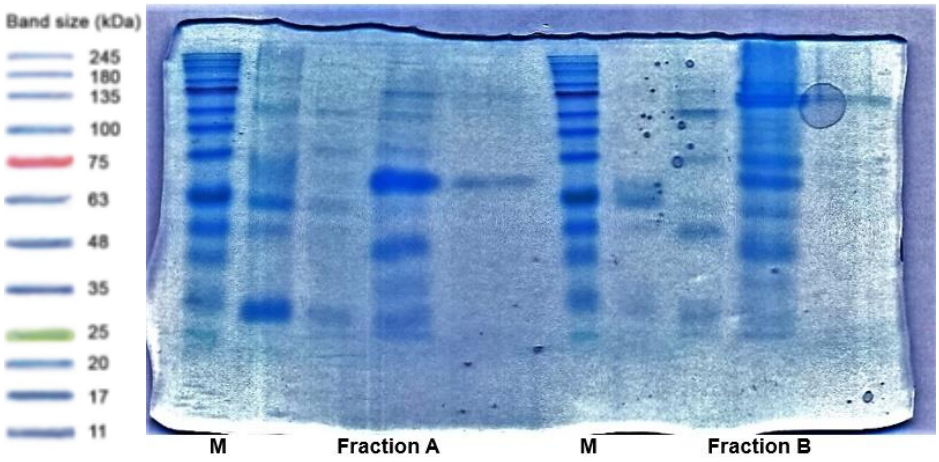

Figure 6.6 – "Fraction A" corresponds to the Fraction A from previous purification, now nominated as Fraction A1. "Fraction B" corresponds to the Fraction B from previous purification, now nominated as Fraction B1. Marker "M" NZYcolour Protein Marker II.

6.7 – Appendix 7: Western Blot analyze of SQR anionic exchange chromatography

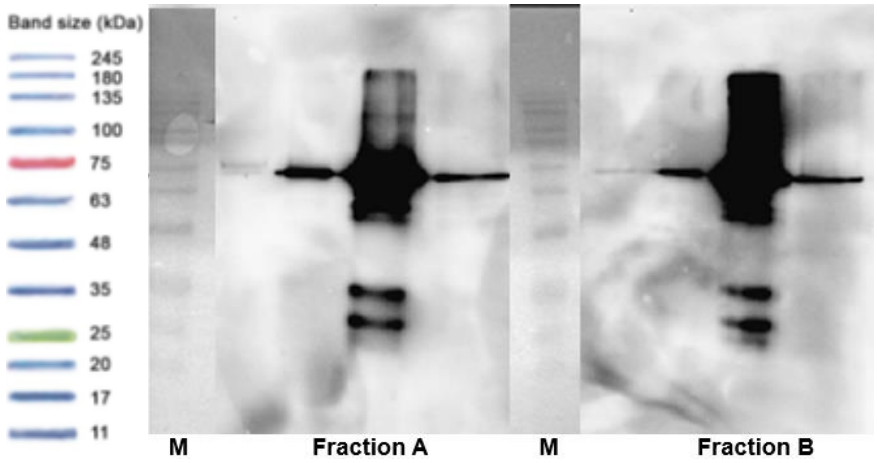

Figure 6.7 - "Fraction A" corresponds to the Fraction A from previous purification, now nominated as Fraction A1. "Fraction B" corresponds to the Fraction B from previous purification, now nominated as Fraction B1. Marker "M" NZYcolour Protein Marker II. WB done with anti-SQR antibody.

6.8 – Appendix 8: SDS-PAGE analyze of SQR molecular exclusion chromatography

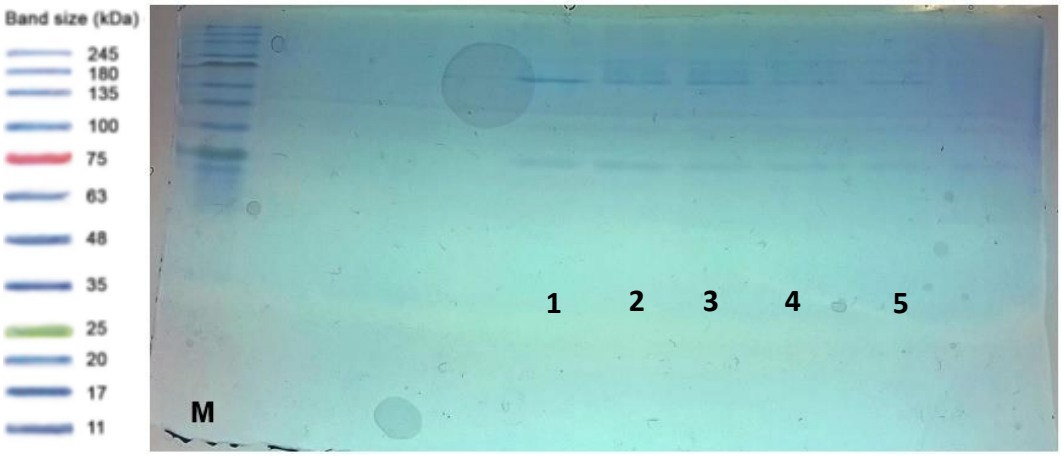

Figure 6.8 – Fraction B1 from previous purification, now nominated Fraction B1B. Fractions from 1-5 pooled and concentrated. Marker "M" NZYcolour Protein Marker II.

6.9 – Appendix 9: Western Blot analyze of SQR molecular exclusion chromatography

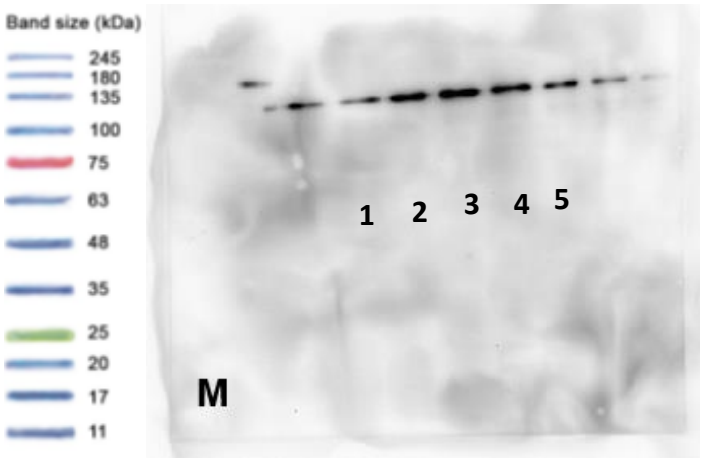

Figure 6.9 - Fraction B1 from previous purification, now nominated Fraction B1B. Fractions from 1-5 pooled and concentrated. Marker "M" NZYcolour Protein Marker II. WB done with anti-SQR antibody.

6.10 – Appendix 10: SDS-PAGE analyze of SQR ResourceQ chromatography

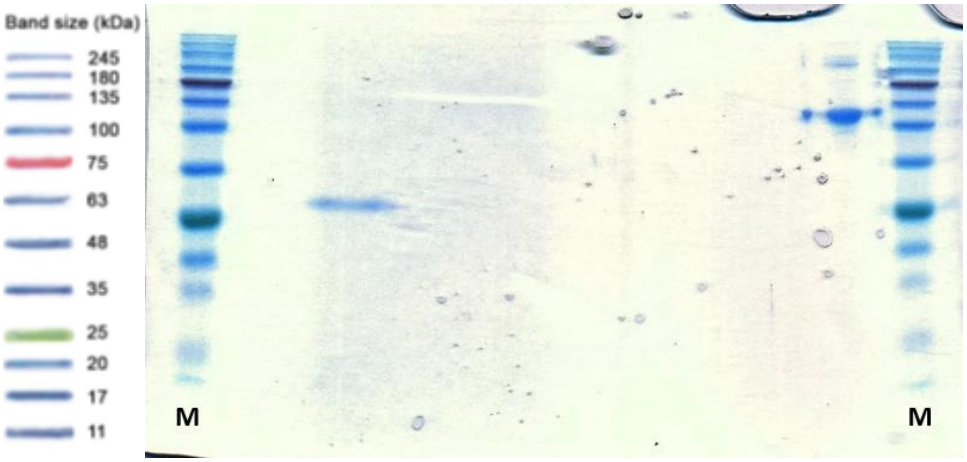

Figure 6.10 – Fraction B1B from previous purification. Marker "M" NZYcolour Protein Marker II.

6.11 – Appendix 11: Western Blot analyze of SQR ResourceQ chromatography

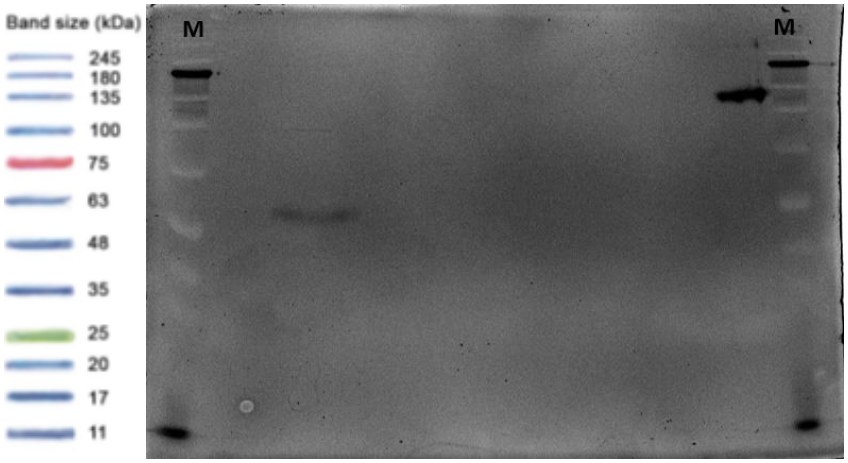

Figure 6.11 - Fraction B1B from previous purification. Marker "M" NZYcolour Protein Marker II. WB done with anti-SQR antibody.